Regeneration and modelling of a phosphorous removal and recovery hybrid ion exchange resin after long term operation with municipal wastewater

Regeneration and modelling of a phosphorous removal and recovery hybrid ion exchange resin after long term operation with municipal wastewater

D. Pinelli, S. Bovina, G. Rubertelli, A. Martinelli, S. Guida, A. Soares, D. Frascari

Abstract

Adsorption represents one of the most promising process for phosphorous (P) removal and recovery from municipal wastewater, but questions about its long-term stability remain. The goals of this work were (i) to assess changes in morphology and adsorption performances of hybrid anion exchanger (HAIX) Layne^{RT} after 2.5 years of operation in a 10 m^3 d^{-1} demonstration plant fed with secondary-treated municipal wastewater, (ii) to optimize the Layne^{RT} regeneration procedure, and (iii) to evaluate the suitability of the ion exchange model to describe P adsorption on Layne^{RT}. Layne^{RT} is composed of hydrated ferric nanoparticles dispersed in a strong base anion exchange resin. Batch and continuous flow adsorption/desorption tests were conducted with the resin used for 2.5 years, regenerated with two alternative solutions: NaOH, reactivating mainly the iron nanoparticles active sites, and NaOH + NaCl, also regenerating the active sites of the ion exchange media. The physicochemical characterization by Scanning Electron Microscope indicated that regeneration by NaOH significantly reduced the deterioration of the resin surface, even after 59 adsorption/desorption cycles. Lab-scale continuous flow tests showed that the resin regenerated with either solution featured P adsorption performances very close to that of the virgin resin. The isotherm tests showed that P adsorption by Layne^{RT} was effectively simulated with the ion exchange model. This study confirms that Layne^{RT} is a durable, resistant and promising media for P recovery from wastewater.

Keywords: phosphorous recovery, adsorption, hybrid anion exchanger, municipal wastewater, isotherm, ion exchange model.

1. INTRODUCTION

Phosphorous (P) is essential for life since it is a key element in DNA and a main nutrient in plant growth. Its widespread usage in chemical fertilisers and the incomplete removal of municipal and industrial wastewater treatment plants leads to severe impacts in aquatic ecosystems. The excessive presence of P in water bodies causes eutrophication in water bodies. Regulation regarding the maximum P concentration in wastewater treatment plant (WWTP) effluents is continuously stricter (Sengupta and Pandit, 2011; Soares, 2020). On the other side, P is a non-renewable resource, primarily obtained from phosphate rock, listed as a critical raw material by the European Union (European Commission, 2014). Municipal wastewater (MWW) is a promising source of P for fertilizer production, since it is widely distributed and continuously available (Schoumans et al., 2015). Thus, P removal and recovery in WWTPs attracted considerable research interest (Egle et al., 2016, 2015; Kehrein et al., 2020).

Adsorption represents one of the most promising processes to remove P from aqueous solutions (Bunce et al., 2018). In secondary wastewater effluents, P is present at 4 – 12 mg_P L^{-1} (Tchobanoglous et al., 2003). Adsorption guarantees full control of the effluent quality and allows P recovery, leading to a final product usable for fertilizer manufacture (Sengupta and Pandit, 2011). In comparison with alternative P recovery technologies, adsorption presents advantages such as operational simplicity, low capital and operational costs (Blaney et al., 2007).

Many studies focused on the development of materials to selectively remove P from MWW (Bunce et al., 2018). Adsorbents used for arsenate can be effectively implemented for P uptake, due to the similar structure of these elements. Research in this field led to the development of hybrid anion exchanger (HAIX) media, in which a strong base macroporous anion exchange resin supports a dispersion of metal oxide nanoparticles (Cumbal et al., 2003). Several researchers attempted to couple

metals with materials that can support the metal nanoparticles (Bunce et al., 2018). Given the relevant costs of HAIX media and the environmental impact associated with their regeneration and final disposal (Huang et al., 2020), the number of adsorption/desorption cycles that can be performed before the resin performances drop significantly, has a relevant impact on the life cycle assessment and operational cost of P recovery. However, studies focused on the long-term testing of P recovery with HAIX media conducted with actual WWTP effluents at a meaningful scale are extremely limited, and further research is needed to assess the economic and environmental sustainability of the process (Drenkova-Tuhtan et al., 2017; Kalaitzidou et al., 2016). A commercial HAIX resin that resulted in interesting P adsorption performances is Layne^{RT}, characterized by hydrated ferric nanoparticles within a strong base anion exchanger with quaternary ammonium functional groups (Boyer et al., 2011; Pan et al., 2009b, 2009a).

The goals of this work were (i) to assess changes in morphology and adsorption of Layne^{RT} after 2.5 years of operation in a 10 m^3 d^{-1} demonstration plant fed with secondary treated municipal wastewater, (ii) to optimize the Layne^{RT} regeneration procedure, (iii) to evaluate the suitability of the ion exchange model to describe P adsorption on Layne^{RT}, and (iv) to determine the relative contribution of iron nanoparticles and of the ion exchange matrix to the P adsorption capacity of Layne^{RT}. To attain these goals, the used Layne^{RT} resin was regenerated by means of two alternative procedures: the first one, performed with NaOH, was aimed at regenerating primarily the iron nanoparticles active sites, whereas the second one, performed with NaOH + NaCl, was aimed at regenerating the active sites of both the iron nanoparticles and the ion exchange support media. The 2 types of regenerated resin were then compared to the virgin resin through physicochemical characterization by Scanning Electron Microscope (SEM). Further to this isotherms conducted with both a P synthetic solution and MWW were conducted to understand the contribution of Fe nanoparticles to the overall P adsorption, and the P adsorption capacity was verified in continuous flow adsorption/desorption tests. This is the first study focused on the understanding of long-term operation and aging in a P recovery process based on the use of a hybrid resin with MWW. In addition, this work applies for the first time the ion exchange model for the simulation of phosphorous removal with a hybrid ion exchanger.

2. MATERIAL AND METHODS

2.1 Adsorbent media characterization

Layne^{RT} was purchased from SolmeteX (Massachusetts, USA). The media had a mean size of 0.69 mm (Martin et al., 2018) (Table S1). Layne^{RT} comprises a strong base anionic ion-exchange resin which supports ferric oxide nanoparticles (Blaney et al., 2007; Cumbal et al., 2003). Details about Layne^{RT} activation and regeneration are in Table S1, Supplementary Material.

The long-term Layne^{RT} resin was obtained after 2.5 years of operation (63 adsorption/desorption cycles) in a 10 m^3 d^{-1} demonstration plant fed with secondary treated municipal wastewater from Cranfield (UK) WWTP (Table S2). The demonstration plant consisted of a 58 L column (resin bed height 0.94 m, total height 1.58 m, column diameter 0.22 m) operated with a 5-minute empty bed contact time (EBCT) (Guida et al., 2021). Resin regeneration was completed with 10 BVs of 2%wt NaOH solution, upon the achievement of a 3 mg_P L^{-1} breakpoint. The same used NaOH solution was re-used as a regenerant multiple times and the phosphate periodically recovered as $Ca_3(PO_4)_2$. After 63 cycles, the used resin was unloaded and used for the tests object of this study.

2.2 Characteristics of MWW and synthetic wastewater

The lab-scale isotherm and continuous flow tests aimed at characterizing the used Layne^{RT} were conducted with two type of wastewaters: i) a synthetic solution, consisting in a K_2HPO_4/KH_2PO_4 mixture (mass ratio 1:2) dissolved in deionized (DI) water, and ii) the effluent of the Bologna (Italy) WWTP (Table S2, Supplementary Material) spiked with the a K_2HPO_4/KH_2PO_4 concentrated

solution (pH 6.8) to reach 7 mg_P L^{-1}, a reasonable P content in a municipal WWTP effluent if no P removal is implemented (EPA, 2007).

2.3 Layne^{RT} regeneration

The used Layne^{RT} resin was regenerated before it was further studied in the lab-scale batch and the 0.17 L lab-scale column continuous flow tests. Two different solutions were used: i) a NaOH 2% w/v solution (0.50 equivalents OH^- L^{-1}), hereinafter named NaOH solution, aimed at regenerating mainly the iron nanoparticles adsorption sites; considering that the affinity for OH^- of strong base anion exchange resins such as Layne^{RT} is 5-85 times lower than that relative to the other main anions present in MWW (DuPont, 2019), this solution is supposed to have a minor regeneration effect on the strong sites of the parent ion exchange (IE) matrix (Martin et al., 2018); ii) a solution of NaOH 2% w/v (0.50 equivalents OH^- L^{-1}) and NaCl 5% w/v (0.86 equivalents Cl^- L^{-1}), named NaOH/NaCl solution; considering the high affinity for Cl^- of strong base anion exchange resins (22 times higher than that for OH^-; DuPont, 2019), and the high concentration of Cl^- equivalents, this solution is supposed to regenerate both the iron nanoparticles and the IE matrix active sites, and possibly to desorb the organic matter adsorbed on the resin. The regeneration tests were conducted in batch mode to pre-treat the resin used for the kinetic and isotherm tests, and in continuous mode to pre-treat the resin used for the column tests.

2.4 Adsorption isotherms

The P adsorption isotherms were performed using the virgin Layne^{RT}, the used resin regenerated with NaOH, and the used resin regenerated with NaOH/NaCl. For each type of resin, both the P synthetic solution and the Bologna WWTP effluent were tested over a wide concentration of P (0 – 1 g L^{-1}). The resin concentration was maintained constant at 1 $g_{dry\ resin}$ L^{-1}, the liquid volume was set to 100 mL. For each isotherm point conducted with WWTP effluent, the desired P initial concentration was reached by mixing 100 mL of effluent with 0.005-1 mL aliquots of different K_2HPO_4/KH_2PO_4 solutions, so as to maintain the effect of dilution of the competing anions at negligible levels (< 1%). In each added solution, the K_2HPO_4:KH_2PO_4 mass ratio was equal to 1:2, in order to maintain the solution pH at 6.8. The vials were placed in a rotatory shaker (200 rpm, 22 °C) for 6 hours, to reach equilibrium. The duration of the experiment was defined on the basis of the outcome of kinetic tests; details on the kinetic tests and the models tested are reported in Table S3, Supplementary Material. The tests were performed in triplicates. The experimental data were interpolated by means of the Langmuir, Freundlich and (limitedly to the test conducted with synthetic P solution) IE models. The model equations and the best-fit procedure are reported in Table S3. The model parameters were estimated by non-linear least squares regression of the calculated P sorbed concentrations to the corresponding experimental values (Frascari et al., 2013).

2.5 Continuous-flow adsorption/desorption breakthrough tests

The column used for the lab-scale breakthrough tests had a total height of 1.26 m, a resin bed height of 0.94 m as in the 58-L demonstration plant and a 13 mm inner diameter. The column total volume resulted 0.167 L. The fluid dynamic behaviour of each adsorption bed was studied before the adsorption experiments by a frontal analysis test conducted with de-ionized water after conditioning the column with 0.05 M NaOH. These tests were aimed at (i) comparing the quality of the packings of the 2 types of regenerated resin with that of the virgin resin, and (ii) assessing the entity of possible flow maldistributions. Details on column design and column packing assessment are in Table S4, Supplementary Material.

The breakthrough tests fed with the Bologna WWTP effluent were conducted at 24-25 °C. During the adsorption step, the wastewater was fed downstream with a Masterflex L/S peristaltic pump. The EBCT was set to 5.2 ± 0.1 min, as in the 58 L pilot plant. Pressure drop and flowrate were measured hourly. Samples at the outlet were taken every 15 minutes. The average PO_4-P inlet concentration was

used to normalize the outlet values. Adsorption tests were continued until the attainment of a 0.80-0.85 outlet normalized concentration.
The P adsorption performances of each tested resin were quantified by means of the following performance indicators, referred to a breakpoint concentration of either 1 or 0.1 $mg_P\ L^{-1}$ and evaluated as described previously (Frascari et al., 2019a, 2016): i) BVs of WWTP effluent fed to the process, defined as (WWTP effluent treated)/(resin BV); ii) P operating capacity, defined as (P mass adsorbed)/(resin mass).
In the regeneration/desorption step, 2 BVs of de-ionized water were eluted to backwash the bed, then 10 BVs of NaOH solution were eluted to regenerate the resin and recover the P-rich product. A 10-minute EBCT was applied. An average sample of the outlet desorbed solution was analyzed. The desorption performance was quantified by means of the desorption yield, assessed as the ratio between the desorbed and adsorbed mass of P.

2.6 Analytical methods and chemical analysis

The analysis of anions (Cl^-, NO_3^-, SO_4^{2-}, PO_4^{3-}) were carried out using an Integrion ion chromatograph (ThermoFisher Scientific, Walthman, Massachusetts) equipped with an IonPacTM AS23 4 x 250 mm column, and an Electrolytically Regenerated Suppressor AERS 500 Carbonate 4 mm, with 4.5 mM sodium carbonate / 0.8 mM sodium bicarbonate as mobile phase. COD was measured spectrophotometrically as described previously (Frascari et al., 2019b). Total organic carbon and BOD_5 were analysed in accordance with Standard Method 5310 (APHA et al., 2017). Total Suspended Solids were determined by filtration with a 0.45 μm ALBET cellulose nitrate membrane filter and weighing. pH was measured by employing an XS Sensors electrode pH GEL HT PRO connected to an EUTECH Instruments PC2700 Series (ThermoFisher Scientific, Walthman, Massachusetts). Samples of fresh and used resin taken from the demonstration plant were analysed at the optical microscope (Optech Microscopes Ltd). Fresh resin as well as resin taken for the column after 16 cycles and 59 cycles were successively analysed at the scanning electron microscope (SEM, Tescan Vega 3, Kohoutovice, Czech Republic), before and after regeneration with NaOH.
The relative average experimental errors, estimated by means of a statistical elaboration of repeated analyses of check standards, resulted equal to 1% for anions concentration and 3-4% for the other parameters. All chemicals were provided by Sigma-Aldrich (Milano, Italy).

3. RESULTS AND DISCUSSION

3.1 Evaluation of the long-term Layne^{RT} performances in the demonstration scale plant

A selection of the P breakthrough curves conducted in the 58 L demonstration scale plant is shown in Fig. S1, Supplementary Material. Even after 63 cycles, it was still possible to maintain an effluent concentration below 0.1 $mg_P\ L^{-1}$, indicating that Layne^{RT} can be used after a long-term operation. However, the prolonged use of the resin decreased the amount of bed volumes treated before breakthrough, indicating a gradual decrease in the resin's adsorption capacity (Guida et al., 2021). According to literature, the HAIX adsorption capacity ranges between 0.29 and 14.4 $mg_P\ g_{dry\ resin}^{-1}$, depending on P wastewater concentration (Bottini and Rizzo, 2012; Muhammad et al., 2019). In this work, with an influent concentration of 5-6 $mg_P\ L^{-1}$ and a 5-minute EBCT, the resin presented a maximum adsorption capacity of 4.1 ± 0.4 $mg_P\ g_{dry\ resin}^{-1}$. The NaOH regenerant solution was replaced with a fresh one when the regeneration efficacy was no longer acceptable. The regenerant was reused up to 8 times with a final concentration of 800 $mg_P\ L^{-1}$. Details about the performances of the 58L pilot plant are reported in Table S5, Supplementary Materials.

3.2 Comparison of the virgin and used resin by Scanning Electron Microscopy

The comparison of the virgin Layne^{RT} with the resin after 16 adsorption/desorption cycles at the optical microscope showed that the used resin was partly covered by a white precipitate (Fig. S2, Supplementary Material). A SEM analysis revealed that the used resin after both 16 and 59 cycles presented a higher level of Si, P and Ca on the surface (Fig. S3). Regeneration with NaOH significantly decreased the level of P from the media surface, indicating that the resin maintained a high regeneration capacity even after 59 cycles.
The iron on the resin surface decreased form 23% (atomic weight) in the virgin resin to about 3% in the regenerated resin after 59 cycles (Fig. S3). However, SEM only analyses a defined point on the resin surface, whereas the larger fraction of the iron nanoparticles – and therefore of Layne's P sorption capacity – lies in the resin macroporous structure (Martin et al., 2009). Further investigations of the total iron content of the used regenerated resin, for example iron elution with a strong acid, were not included in this work, as the results of the batch and continuous flow tests performed both in the 58 L plant and in the 0.167 L laboratory column demonstrated that after 63 adsorption/desorption cycles Layne^{RT} maintained a high selectivity and sorption capacity towards P. The SEM images further indicated that, even though the surface of the used resin beads appeared damaged and partly collapsed after both 16 and 59 cycles, regeneration with NaOH was capable to restore the beads shape to a condition quite close to that of the virgin Layne^{RT} (Fig. S4, Supplementary Materials).

3.3 Regeneration of the used Layne^{RT} resin

Before the lab-scale tests of used Layne^{RT} characterization, the resin used during 63 cycles conducted with Cranfield WWTP effluent was regenerated in both batch and continuous flow mode, and the NaOH and NaOH/NaCl regenerants were analyzed. The ratio between the P and COD amounts desorbed and the dry resin mass are presented in Table S6, Supplementary Material. In both the batch and continuous flow tests, the mass of P desorbed with the two regeneration solutions did not result significantly different (*t* test, significance level 0.05), suggesting that in these WWTP effluent tests, due to the strong competition exerted by high concentrations of other anions, phosphate was adsorbed mostly by the nanoparticles, and only marginally on the IE active sites of the polymeric matrix. On the other hand, in both types of regeneration, the amount of COD released using the NaOH/NaCl solution was 16-19 times when compared with NaOH only. This suggests that NaCl displaced organic matter that was trapped by the active sites of the IE matrix.

3.4 Adsorption isotherms

Adsorption kinetic tests, aimed at asserting the adsorption equilibrium time between the liquid and solid phase, were performed both with a synthetic P solution and with the Bologna WWTP effluent (Table S2). Based on these results, the equilibrium time for the subsequent isotherm tests was cautiously set at 6 h. Details on the kinetic tests are reported in Tables S2, S7 and S8, Supplementary Material.
The adsorption isotherms were conducted with the virgin Layne^{RT} resin and with the two types of used regenerated resin. The results are shown in Fig. 1a (synthetic solution) and Fig. 1b (WWTP effluent). The experimental data were fitted with the Langmuir, Freundlich and IE model. The IE model could not be applied to the tests conducted with the WWTP effluent, as it contains several anions in addition to P (Table S2). The estimated model parameters are shown in Table 1. The curves obtained with the Freundlich model presented the best fitting to the experimental data (Fig. 1). The Freundlich model was thus used to estimate the sorbed concentration in equilibrium with a liquid phase concentration of 7 $mg_P\ L^{-1}$ (Table 1), a reasonable concentration for the effluent of a WWTP in which no P removal is implemented (EPA, 2007).
Fig. 1 shows that, at low P concentrations, all the isotherms are very steep, i.e. highly favourable, confirming that Layne^{RT} has a strong affinity to P. Fig. 1 and Table 1 also show that the switch from

synthetic solution to real WWTP effluent determined a 65-70% drop in P adsorption performance. This drop can be ascribed to the presence of other anions (primarily Cl^- 150 mg L^{-1} and SO_4^{2-} 104 mg L^{-1}; Table S2) competing with P mainly for the IE matrix active sites, whereas P sorption on the iron nanoparticles is supposed to be not significantly affected by the presence of competing anions (Martin et al., 2018). This result is in agreement with the findings of Pan et al. (2009b), that report that an increase in sulphate concentration from 0 to 100 mg L^{-1} led to a 58% drop in phosphate adsorption on similar HAIX resins (HFO-201 and ArsenX^{np}).

With both the synthetic solution and the WWTP effluent, the P adsorption capacity of the used resin regenerated with NaOH was lower than when the resin was regenerated with NaOH/NaCl, which in turn was lower than that of the virgin resin (Fig. 1). The drop in P adsorption capacity was more accentuated in the synthetic solution tests than in the WWTP effluent tests.

A *t* test (significance level 0.05) was used to assess the statistical significance of the observed differences in the sorbed P concentrations in equilibrium with 7 mg_P L^{-1} in the liquid (Table 1). The analysis showed that, for the synthetic solution, in the case of NaOH regeneration a statistically significant drop in adsorption performance was observed in comparison to the virgin resin, whereas the NaOH/NaCl test resulted equivalent to the virgin resin test. Conversely, for the WWTP effluent, the data obtained after NaOH/NaCl regeneration, those found after NaOH regeneration and those of the virgin resin did not result statistically different. These results can be explained by considering that, in the synthetic solution tests, the lack of competing anions leads to a not negligible fraction of P sorbed on the IE active sites; thus, the regeneration of the IE sites performed mainly by the Cl^- anions has a significant effect on the overall P sorption capacity, and the difference between the performances of the NaCl/NaOH-regenerated resin and the NaOH-regenerated resin results statistically significant. Conversely, in the WWTP effluent isotherms, due to the presence of high concentrations of anions competing with P for the IE active sites, the fraction of P sorbed on the latter is small; therefore, the regeneration of the IE sites performed mainly by the Cl^- anions of the NaCl/NaOH solution has a minor effect on the overall P sorption capacity. This result is in agreement with the outcome of the regeneration tests performed directly on the used resin sampled from the 58 L plant after 63 adsorption/desorption cycles performed with WWTP effluent, that led to equal amounts of P desorbed with NaOH and with NaCl/NaOH (section 3.3). A tentative estimation of the IE matrix contribution to the total sorbent capacity towards P in the WWTP effluent tests was conducted on the basis of the asymptotic solid-phase concentrations estimated by means of the Langmuir model ($C_{s,\infty}$, Table 1). The IE contribution resulted equal to 13% of the virgin resin capacity, equal to 0.56 meq_P g^{-1}. The residual 87% can be assumed as an estimate of the additional P sorption capacity due to the iron nanoparticles. These results, that confirm the crucial role played by metal nanoparticles in P recovery with hybrid resins, are in good agreement with the findings of Martin et al. (2018) who estimated that – in the presence of competing anions - the fraction of P adsorbed by the resin via IE is 10% of the total resin capacity.

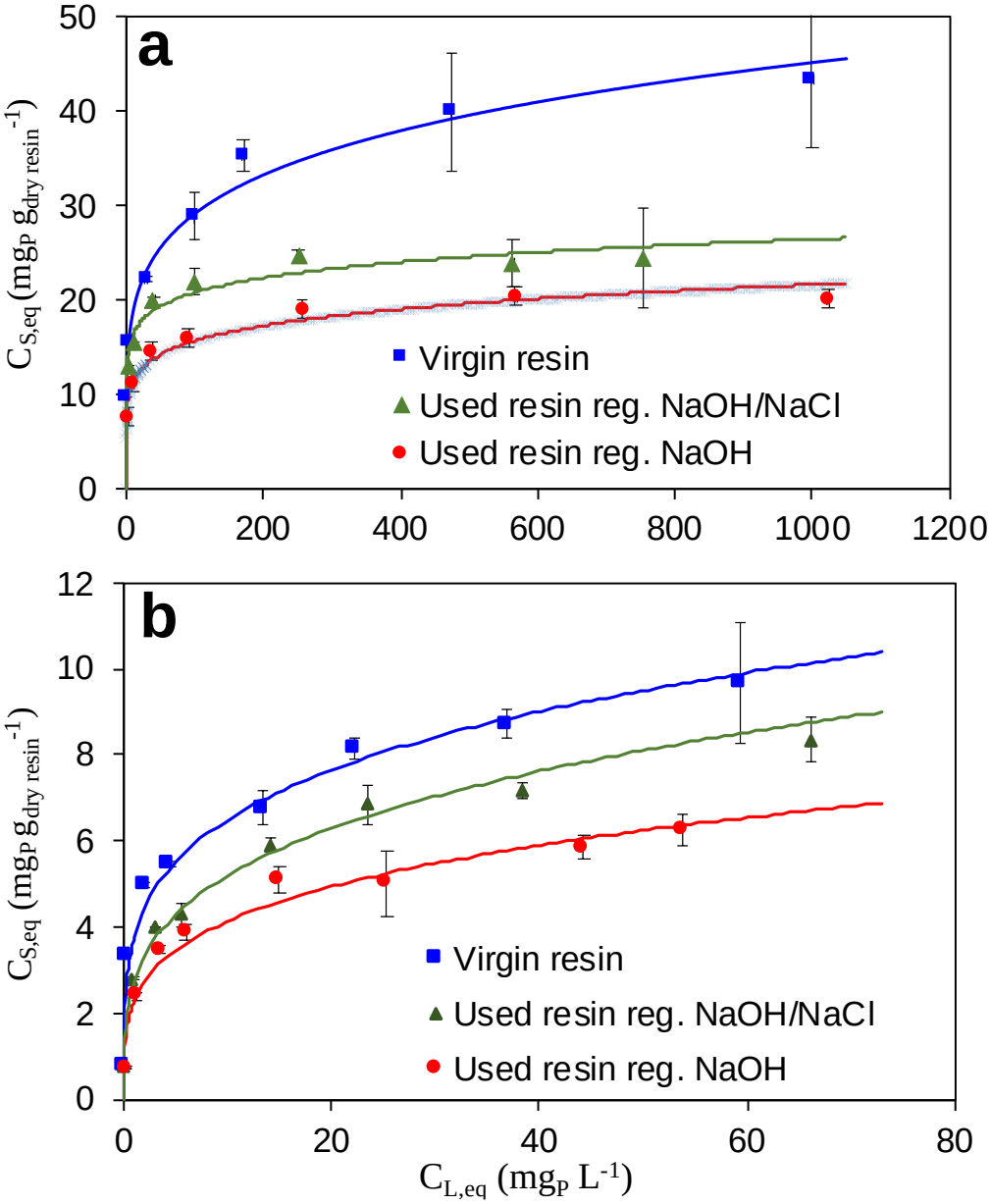

Fig. 1 - P adsorption isotherms, experimental data and Freundlich model best fitting curves, with a) synthetic P solution, b) actual municipal wastewater effluent spiked with phosphate salts. $C_{L,eq}$: liquid-phase P concentration at equilibrium (mg_P L^{-1}); $C_{S,eq}$: solid-phase P concentration at equilibrium (mg_P $g_{dry\ resin}^{-1}$).

Table 1
Isotherm fitting with the Freundlich, Langmuir and IE models. Best-fitting model parameters and P adsorption capacity in equilibrium with a liquid phase concentration of 7 $mg_P\ L^{-1}$.

			Synthetic Solution			Bologna WWTP effluent		
	Parameter	Units	Virgin resin	Resin reg. NaOH[a]	Resin reg. NaOH/NaCl[b]	Virgin resin	Resin reg. NaOH[a]	Resin reg. NaOH/NaCl[b]
IE model	Q	$mg_P\ g_{dry\ resin}^{-1}$	42 ± 7	20 ± 1	26 ± 2	[c]	[c]	[c]
		$meq_P\ g_{dry\ resin}^{-1}$ [d]	2.7 ± 0.5	1.3 ± 0.1	1.7 ± 0.1	[c]	[c]	[c]
	K_{eq}	-	1.2 ± 1.1	1.5 ± 0.6	1.4 ± 0.6	[c]	[c]	[c]
	R^2	-	0.87	0.94	0.85	[c]	[c]	[c]
Langmuir	$C_{s\infty}$	$mg_P\ g_{dry\ resin}^{-1}$	39 ± 8	19 ± 2	23 ± 2	8.7 ± 1.4	6.0 ± 0.6	7.2 ± 1.0
		$meq_P\ g_{dry\ resin}^{-1}$ [d]	2.5 ± 0.5	1.2 ± 0.1	1.5 ± 0.1	0.56 ± 0.09	0.39 ± 0.04	0.46 ± 0.07
	K_{eq}	$L\ mg_P^{-1}$	0.066 ± 0.081	0.17 ± 0.11	0.19 ± 0.14	0.70 ± 0.67	0.40 ± 0.18	0.45 ± 0.31
	R^2	-	0.81	0.89	0.83	0.88	0.96	0.94
Freundlich	n	-	5.3 ± 1.0	7.1 ± 2.0	10 ± 3	4.3 ± 1.3	3.9 ± 1.1	3.6 ± 0.9
	K_F	$mg_P^{1-1/n}\ L^{1/n}\ g_{dry\ resin}^{-1}$	12 ± 2	8.2 ± 1.6	13 ± 2	3.8 ± 0.8	2.3 ± 0.5	2.8 ± 0.5
	R^2	-	0.98	0.94	0.92	0.96	0.96	0.98
$C_{S,P}$ @ $C_{L,P}$ = 7 mg L^{-1} [e]		$mg_P\ g_{dry\ resin}^{-1}$	18 ± 1	11 ± 1	16 ± 1	6.0 ± 1.0	3.8 ± 1.2	4.7 ± 1.1
		$meq_P\ g_{dry\ resin}^{-1}$ [d]	1.1 ± 0.1	0.7 ± 0.1	1.0 ± 0.1	0.39 ± 0.07	0.24 ± 0.08	0.30 ± 0.07

[a] Used resin regenerated with NaOH 2% solution.
[b] Used resin regenerated with NaOH 2% + NaCl 5% solution.
[c] The IE is not applicable to the tests with WWTP effluent, where multiple anions are present.
[d] To calculate the equivalents, on the basis of the MWW pH equal to about 7, phosphate was considered a bivalent anion.
[e] Solid phase concentration calculated with the Freundlich model, in equilibrium with 7 $mg_P\ L^{-1}$ in the liquid phase.

In the tests conducted with synthetic solution the IE model resulted in a satisfactory fit of the experimental behavior of the Layne^{RT} resin (R^2 = 0.85 – 0.94), despite the fact that this sorbent is not a pure IE resin (Fig. S5, Supplementary Materials). Furthermore, the asymptotic solid concentrations predicted by IE model (Q) resulted in good agreement with the corresponding value provided by the Langmuir model ($C_{s,\infty}$; Table 1). This represents the first study in which the adsorption behaviour of a hybrid ion exchanger is successfully simulated with an IE model.

3.6 Continuous adsorption / desorption breakthrough tests in the lab-scale column

As a preliminary step, a fluid-dynamic analysis was performed on the adsorption columns packed with the three resins tested in the isotherm batch tests: virgin resin, used resin regenerated with NaOH and used resin regenerated with NaOH/NaCl. The fluid-dynamic analysis resulted in a good quality of the three packings. The porosities of the 3 resins were very close to each other, with an average value of 76 ± 3%, indicating that the aging of the Layne^{RT} resin did not had an impact on the resin porosity. Overall, this analysis indicated that – despite the quite low (column inner diameter)/(particle mean size) ratio, equal to 19 - the continuous flow adsorption / desorption tests were conducted in a column characterized by an acceptable fluid-dynamic behaviour with negligible wall effects. The cumulative retention time curves obtained in the frontal analysis tests are shown in Fig. S6 and discussed in Table S9, Supplementary Material.

3.6.1 Adsorption breakthrough curves

After the fluid-dynamic tests, the columns packed with the 3 forms of the Layne^{RT} resin were used for an adsorption / desorption breakthrough test fed with actual effluent of the Bologna WWTP (Table S2). All the 3 tests were continued until resin saturation (440 – 450 BVs); in the 2 tests conducted with the used resins the monitoring of the main anions in the outlet was continued only until a P effluent concentration equal to 1.4 – 1.5 mg_P L^{-1} (20% of the inlet concentration of 7 mg_P L^{-1}). The operational conditions of the 3 tests and selected performance parameters are in Table 2, and the results of the adsorption tests are in Fig. 2. The tests were compared in terms of wastewater BVs fed and P operating capacity when the breakpoint concentrations were equal to 1 mg_P L^{-1} and 0.1 mg_P L^{-1} (Table 2). The former value corresponds to the limit imposed by the European Directive 91/271/EEC for WWTPs with > 100,000 population equivalent, whereas the latter is a lower limit that has already been enforced in selected regions in the USA, and sensitive areas in Europe.

Table 2
Operating conditions and performance parameters for the adsorption breakthrough tests conducted with the virgin resin and the two types of used resin, shown in Fig. 2 and Fig. S7.

		Virgin resin		Used resin regenerated with NaOH		Used resin regenerated with NaOH/NaCl	
Operational conditions	Bed volume (BV_{resin}, mL)	125		125		125	
	Mass of dry resin (g)	38		38		38	
	Empty bed contact time (EBCT, min)	5.13 ± 0.02		5.15 ± 0.02		5.25 ± 0.02	
	Superficial velocity (v_{sup} , m h^{-1})	11.0 ± 0.1		10.9 ± 0.1		10.7 ± 0.1	
	Bed volumes/h (BV h^{-1}, h^{-1})	11.7 ± 0.3		11.6 ± 0.3		11.4 ± 0.2	
	Inlet P conc. (mg L^{-1})	7.1 ± 0.2		6.6 ± 0.2		6.9 ± 0.1	
Performance parameters	*P breakpoint value*	*0.1 mg L^{-1}*	*1 mg L^{-1}*	*0.1 mg L^{-1}*	*1 mg L^{-1}*	*0.1 mg L^{-1}*	*1 mg L^{-1}*
	WWTP effluent treated ($V_{treated\ MWW}/BV_{resin}$, -)	219 ± 9	251 ± 10	203 ± 8	242 ± 10	231 ± 9	265 ± 10
	P operating capacity ($mg_P\ g_{dry\ resin}^{-1}$)	4.7 ± 0.2	5.4 ± 0.2	4.4 ± 0.2	5.2 ± 0.2	5.2 ± 0.2	5.9 ± 0.3
	($meq_P\ g_{dry\ resin}^{-1}$)	0.30 ± 0.01	0.35 ± 0.02	0.28 ± 0.01	0.33 ± 0.02	0.34 ± 0.02	0.38 ± 0.02

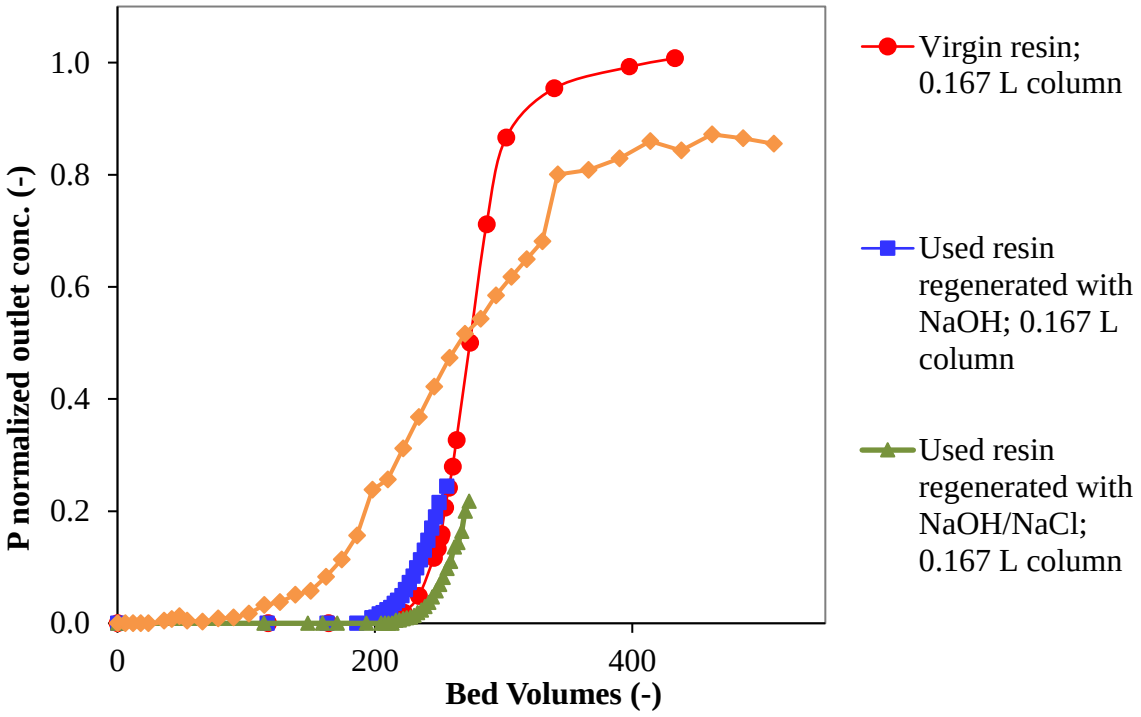

Fig. 2 - Breakthrough curves obtained in the lab-scale (0.17 L) and demonstration scale (58 L) columns, shown as outlet P normalized concentration versus the BVs fed to the column. Initial P concentrations were: 7.1 ± 0.2 $mg_P\ L^{-1}$ for virgin resin, 6.6 ± 0.2 $mg_P\ L^{-1}$ for the used resin regenerated with NaOH and 6.9 ± 0.1 $mg_P\ L^{-1}$ for used resin regenerated with NaOH/NaCl.

Fig. 2 shows that the breakthrough curves obtained with the virgin resin and with the two forms of regenerated resin are very similar. This observation is confirmed by the fact that, for all the performance parameters (BVs fed and P operating capacity, at both 1 and 0.1 $mg_P\ L^{-1}$; Table 2), no statistically significant differences were found (*t* test, significance level 0.05). This is aligned with the isotherms conducted with WWTP effluent, where no statistically significant differences were found between the 3 resins (Table 1). This result indicates that, after a long-term operation with actual WWTP effluent, Layne^{RT} can be effectively regenerated with either NaOH or NaOH/NaCl, without any significant loss of its P adsorption capacity, at least at the low P concentrations of interest in the case of P recovery from MWW.

The P operating capacities obtained with the 3 forms of Layne^{RT} (5.2 – 5.9 $mg_P\ g_{dry\ resin}^{-1}$) are in agreement with those found previously, in continuous flow tests of P adsorption from MWW using hybrid resins analogous to Layne^{RT} (2 – 6 $mg_P\ g_{dry\ resin}^{-1}$; Kalaitzidou et al., 2016; Martin et al., 2013; Sengupta and Pandit, 2011). In virgin resin test, the effluent monitoring up to resin saturation allowed to assess the P adsorption yield, equal to 99.1%, and the fraction of resin bed utilized at the 1 $mg_P\ L^{-1}$ breakpoint. The latter parameter resulted equal to 90% of the total capacity at saturation, confirming the high P adsorption performance of Layne^{RT}.

For comparison, a representative P breakthrough curve obtained after 42 adsorption/desorption cycles in the demonstration scale plant (Fig. 2) shows an early breakpoint in comparison with the tests conducted in the 0.167 L columns packed with the 3 resins. The number of BVs corresponding to the 1 $mg_P\ L^{-1}$ breakpoint was 23% lower, and the breakthrough curve was significantly less steep, corresponding to a larger mass transfer zone, and therefore to a lower efficiency in the utilization of the resin bed. It is reasonable to assume that the smaller lab-scale column presented a better fluid-dynamic behaviour and a lower longitudinal dispersion. Indeed, it should be considered that in the 0.167 columns the adsorption bed was used only once, whereas in the case of the demonstration plant, the periodic up-flow regeneration procedure conferred partial fluidization of the bed, that can significantly change its fluid-dynamics.

The breakthrough curves of the main competing anions present in the WWTP effluent, namely chloride (feed concentration = 150 mg L^{-1}), nitrate (6.7 mg L^{-1}) and sulphate (104 mg L^{-1}), are shown in Fig. S7 in Supplementary Material for the representative case of the used resin regenerated with NaOH. The curves obtained with the other two resins presented similar trends and the same order by which the anions are eluted: the less retained was chloride, followed by nitrate, sulphate and finally phosphate. This order is aligned with the expectation for a strong IE anion resin such as the polymeric matrix of Layne^{RT} (Perry and Green, 2008). In the resin regenerated with NaOH, the BVs required to reach a breakpoint equal to 10% of the inlet concentration were equal to 230 for P, 160 for sulphate, 125 for nitrate and only 35 for chloride, confirming the high selectivity of Layne^{RT} for P even after 63 adsorption / desorption cycles conducted with MWW. The used resin regenerated with NaOH/NaCl presented a delayed elution of sulphate in comparison with NaOH regeneration. This difference can be ascribed to the higher capacity of polymeric matrix IE sites that were regenerated by the Cl^- ions.

3.6.2 Desorption continuous flow tests

After each breakthrough test, the adsorption bed was regenerated with 10 BVs of a 2% NaOH solution. The resulting relative anion abundances are shown in Table 3 in terms of (equivalents of a given anion)/(total anion equivalents). All the 3 tested forms of Layne^{RT} were capable to concentrate P, and the regenerant contained 20–22% relative abundance in P, starting from an influent MWW with a 6% P relative abundance. The analysis of the P/SO_4^{2-} and P/Cl^- ratios in the WWTP effluent fed to the process and in the desorbed product confirmed the high affinity of all the forms of Layne^{RT} for P (Table 3). The high Cl^- content of the product obtained from the resin initially regenerated with NaOH/NaCl can be ascribed to the fact that the residual Cl^- in the resin at the end of the adsorption process is released when the resin is treated with NaOH. Table 3 shows that the 2 types of regenerated

Layne^{RT} were similar to the virgin resin in terms of capacity to retain P and concentrate it in the desorbed product.

The compositions of the desorbed solutions were used to assess the total anion adsorption capacity and the P adsorption capacity of the 3 forms of Layne^{RT} (Table 3). The total capacity of the NaOH/NaCl-regenerated resin (2.1 $meq_P\ g_{dry\ resin}^{-1}$) was not statistically different from that of the virgin resin (2.0 $meq_P\ g_{dry\ resin}^{-1}$; *t* test, 0.05 significance level) whereas the total capacity of the NaOH-regenerated Layne^{RT} was 15% lower and statistically different from its virgin state. As shown in Table 3, these desorption-based estimates of the Layne^{RT} total capacity are in reasonable agreement with the isotherms conducted with the synthetic solution, that represent the best way to estimate the total resin capacity in the absence of anion competition. A more detailed discussion of the desorption results is reported in Table S10, Supplementary Material.

Table 3

Characterization of the regenerant, desorbed product, recovered after regeneration with 10 BVs of a 2% NaOH solution, and comparison of the adsorption capacities obtained from the isotherms, adsorption tests and desorption tests.

Parameter		Units	Virgin resin	Resin regenerated with NaOH	Resin regenerated with NaOH/NaCl
Relative anion abundance	Cl^-	[a]	0.14	0.18	0.34
	NO_3^-	[a]	0.01	0.01	0.005
	SO_4^{2-} [b]	[a]	0.64	0.59	0.46
	P [b]	[a]	0.21	0.22	0.20
P/other anions concentration ratios	P/SO_4^{2-}: influent MWW	[c]	0.22	0.22	0.23
	P/SO_4^{2-}: desorbed product	[c]	0.33	0.37	0.43
	P/Cl^-: influent MWW	[c]	0.12	0.12	0.13
	P/Cl^-: desorbed product	[c]	1.47	1.19	0.59
Layne^{RT} total capacity	Isotherm tests[d]	$meq_P\ g_{dry\ resin}^{-1}$	2.7 ± 0.5	1.3 ± 0.1	1.7 ± 0.1
	Desorption tests[e]	$meq_P\ g_{dry\ resin}^{-1}$	2.0 ± 0.1	1.7 ± 0.1	2.1 ± 0.1
Layne^{RT} P capacity	Isotherm tests[f]	$meq_P\ g_{dry\ resin}^{-1}$	0.39 ± 0.07	0.24 ± 0.08	0.30 ± 0.07
	Adsorption column tests[g]	$meq_P\ g_{dry\ resin}^{-1}$	0.35 ± 0.02	0.33 ± 0.02	0.38 ± 0.02
	Desorption column tests[h]	$meq_P\ g_{dry\ resin}^{-1}$	0.42 ± 0.01	0.38 ± 0.06	0.41 ± 0.02

[a] (equivalents of each anion) / (total anion equivalents).

[b] To calculate the equivalents, on the basis of the MWW pH equal to about 7, both sulphate and phosphate were considered bivalent anions.

[c] (P equivalents) / (SO_4^{2-} or Cl^- equivalents).

[d] Estimate obtained from the isotherms conducted with P-rich synthetic solution, IE model, at infinite concentration in the liquid (*Q*; Table 1)

[e] (Sum of the equivalents of P, Cl^-, NO_3^- and SO_4^{2-} present in the desorbed product) / (mass of dry resin).

[f] Estimate obtained from the isotherms conducted with WWTP effluent, Freundlich model, at 7 $mg_P\ L^{-1}$ in the liquid (Table 1).

[g] Estimate obtained from the adsorption tests at the 1 $mg_P\ L^{-1}$ breakpoint (Table 2).

[h] (P equivalents in the desorbed product) / (mass of dry resin).

4. CONCLUSIONS

- Layne^{RT} was successfully used during 63 P adsorption/desorption cycles in a 10 m^3 d^{-1} demonstration plant fed with secondary treated wastewater. The resin periodic regeneration with an NaOH solution allowed to maintain fairly constant P adsorption performances with a maximum capacity of 4.1 mg_P $g_{dry\ resin}^{-1}$.
- Lab-scale isotherms and continuous flow tests of P adsorption/desorption conducted with virgin resin and with the used resin regenerated by NaOH or NaOH/NaCl showed that both regeneration procedures lead to a complete recovery of the P adsorption capacity and selectivity of Layne^{RT}. Regeneration with only NaOH resulted to be the recommended one for P recovery from MWW.
- The SEM analysis of the virgin and used Layne^{RT} revealed that regeneration by NaOH was capable to (i) eliminate almost completely the surface fouling and precipitates of the resin surface and (ii) lead to a drastic reduction of the P content on the resin surface even after 59 adsorption/desorption cycles, indicating its ability to regenerate the scaffold part of the resin too.
- The isotherm tests indicated that P adsorption in both virgin and used Layne^{RT} was effectively described by the ion exchange model. To the authors' knowledge, this represents the first study in which the ion exchange model was successfully used to simulate the adsorption behaviour of a hybrid ion exchanger.

Overall, these findings indicate that Layne^{RT} can be effectively regenerated even after a long period of operation with MWW. The ability to use the resin for prolonged periods of time in WWTPs will have a positive impact on the LCA and cost analysis of the process, confirming that Layne^{RT} is a durable and promising media for P recovery from wastewater.

Acknowledgments

The authors acknowledge the Partnership on Research and Innovation in the Mediterranean Area (PRIMA) Programme for funding the FIT4REUSE project under grant agreement number 1823 (https://fit4reuse.org/). The PRIMA Programme is supported under Horizon 2020, the European Union's Framework Programme for Research and Innovation. S. Guida and A. Soares received funding from the Europe Union's Horizon 2020 research and innovation programme under grant agreement number 690323.

DATA AVAILABILITY

Research data underlying this manuscript have been published in the AMS Acta Institutional Research Repository (doi: 10.6092/unibo/amsacta/6627).

Appendix A. Supplementary data

Supplementary data to this article can be found online.

References

APHA, AWWA, WEF. Standard Methods for the Examination of Water and Wastewater. Am Public Heal Assoc 2017:1–5.

Blaney LM, Cinar S, SenGupta AK. Hybrid anion exchanger for trace phosphate removal from water and wastewater. Water Res 2007;41:1603–13. https://doi.org/10.1016/j.watres.2007.01.008.

Bottini A, Rizzo L. Phosphorus Recovery from Urban Wastewater Treatment Plant Sludge Liquor by Ion Exchange. Sep Sci Technol 2012;47:613–20.

https://doi.org/10.1080/01496395.2011.627904.
Boyer TH, Persaud A, Banerjee P, Palomino P. Comparison of low-cost and engineered materials for phosphorus removal from organic-rich surface water. Water Res 2011;45:4803–14. https://doi.org/10.1016/j.watres.2011.06.020.
Bunce JT, Ndam E, Ofiteru ID, Moore A, Graham DW. A review of phosphorus removal technologies and their applicability to small-scale domestic wastewater treatment systems. Front Environ Sci 2018;6:1–15. https://doi.org/10.3389/fenvs.2018.00008.
Cumbal L, Greenleaf J, Leun D, SenGupta AK. Polymer supported inorganic nanoparticles: Characterization and environmental applications. React Funct Polym 2003;54:167–80. https://doi.org/10.1016/S1381-5148(02)00192-X.
Drenkova-Tuhtan A, Schneider M, Franzreb M, Meyer C, Gellermann C, Sextl G, et al. Pilot-scale removal and recovery of dissolved phosphate from secondary wastewater effluents with reusable ZnFeZr adsorbent @ Fe3O4/SiO2 particles with magnetic harvesting. Water Res 2017;109:77–87. https://doi.org/10.1016/j.watres.2016.11.039.
Dupont. Ion Exchange Resins Selectivity. Tech Fact No. 45-D01458-en, Rev. 2. Wilmington (DA): 2019.
Egle L, Rechberger H, Krampe J, Zessner M. Phosphorus recovery from municipal wastewater: An integrated comparative technological, environmental and economic assessment of P recovery technologies. Sci Total Environ 2016;571:522–42. https://doi.org/10.1016/j.scitotenv.2016.07.019.
Egle L, Rechberger H, Zessner M. Overview and description of technologies for recovering phosphorus from municipal wastewater. Resour Conserv Recycl 2015;105:325–46. https://doi.org/10.1016/j.resconrec.2015.09.016.
EPA. Advanced wastewater treatment to achieve low concentration of phosphorus. 2007. https://doi.org/EPA 910-R-07-002.
European Commission. Communication from the commission: on the review of the list of critical raw materials for the EU and the implementation of the raw materials initiative. Brussels: 2014. https://doi.org/10.1016/B978-0-323-60984-5.00062-7.
Frascari D, Bacca AEM, Zama F, Bertin L, Fava F, Pinelli D. Olive mill wastewater valorisation through phenolic compounds adsorption in a continuous flow column. Chem Eng J 2016;283:293–303. https://doi.org/10.1016/j.cej.2015.07.048.
Frascari D, Molina Bacca AE, Wardenaar T, Oertlé E, Pinelli D. Continuous flow adsorption of phenolic compounds from olive mill wastewater with resin XAD16N: life cycle assessment, cost–benefit analysis and process optimization. J Chem Technol Biotechnol 2019a;94:1968–81. https://doi.org/10.1002/jctb.5980.
Frascari D, Rubertelli G, Arous F, Ragini A, Bresciani L, Arzu A, et al. Valorisation of olive mill wastewater by phenolic compounds adsorption: Development and application of a procedure for adsorbent selection. Chem Eng J 2019b;360:124–38. https://doi.org/10.1016/j.cej.2018.11.188.
Frascari D, Zanaroli G, Bucchi G, Rosato A, Tavanaie N, Fraraccio S, et al. Trichloroethylene aerobic cometabolism by suspended and immobilized butane-growing microbial consortia: A kinetic study. Bioresour Technol 2013;144:529–38. https://doi.org/10.1016/j.biortech.2013.07.006.
Guida S, Rubertelli G, Jefferson B, Soares A. Demonstration of ion exchange technology for phosphorus removal and recovery from municipal wastewater. Chem Eng J 2021;420:129913. https://doi.org/10.1016/j.cej.2021.129913.
Huang X, Guida S, Jefferson B, Soares A. Economic evaluation of ion-exchange processes for nutrient removal and recovery from municipal wastewater. Npj Clean Water 2020;3. https://doi.org/10.1038/s41545-020-0054-x.
Kalaitzidou K, Mitrakas M, Raptopoulou C, Tolkou A, Palasantza PA, Zouboulis A. Pilot-Scale Phosphate Recovery from Secondary Wastewater Effluents. Environ Process 2016;3:5–22. https://doi.org/10.1007/s40710-016-0139-1.
Kehrein P, Van Loosdrecht M, Osseweijer P, Garfí M, Dewulf J, Posada J. A critical review of

resource recovery from municipal wastewater treatment plants-market supply potentials, technologies and bottlenecks. Environ Sci Water Res Technol 2020;6:877–910. https://doi.org/10.1039/c9ew00905a.
Martin BD, De Kock L, Gallot M, Guery E, Stanowski S, MacAdam J, et al. Quantifying the performance of a hybrid anion exchanger/adsorbent for phosphorus removal using mass spectrometry coupled with batch kinetic trials. Environ Technol (United Kingdom) 2018;39:2304–14. https://doi.org/10.1080/09593330.2017.1354076.
Martin BD, De Kock L, Stephenson T, Parsons SA, Jefferson B. The impact of contactor scale on a ferric nanoparticle adsorbent process for the removal of phosphorus from municipal wastewater. Chem Eng J 2013;215–216:209–15. https://doi.org/10.1016/j.cej.2012.11.006.
Martin BD, Parsons SA, Jefferson B. Removal and recovery of phosphate from municipal wastewaters using a polymeric anion exchanger bound with hydrated ferric oxide nanoparticles. Water Sci Technol 2009;60:2637–45. https://doi.org/10.2166/wst.2009.686.
Tchobanoglous G, Burton FL, Stensel HD, Metcalf & Eddy Inc. Wastewater Engineering: Treatment and Reuse. 4th ed. New-York: McGraw-Hill; 2003.
Muhammad A, Soares A, Jefferson B. The impact of background wastewater constituents on the selectivity and capacity of a hybrid ion exchange resin for phosphorus removal from wastewater. Chemosphere 2019;224:494–501. https://doi.org/10.1016/j.chemosphere.2019.01.085.
Pan Bingjun, Pan Bingcai, Zhang W, Lv L, Zhang Q, Zheng S. Development of polymeric and polymer-based hybrid adsorbents for pollutants removal from waters. Chem Eng J 2009a;151:19–29. https://doi.org/10.1016/j.cej.2009.02.036.
Pan Bingjun, Wu J, Pan Bingcai, Lv L, Zhang W, Xiao L, et al. Development of polymer-based nanosized hydrated ferric oxides (HFOs) for enhanced phosphate removal from waste effluents. Water Res 2009b;43:4421–9. https://doi.org/10.1016/j.watres.2009.06.055.
Perry R, Green D. Perry's Chemical Engineers' Handbook. 8th ed. New York: McGraw-Hill; 2008.
Schoumans OF, Bouraoui F, Kabbe C, Oenema O, van Dijk KC. Phosphorus management in Europe in a changing world. Ambio 2015;44:180–92. https://doi.org/10.1007/s13280-014-0613-9.
Sengupta S, Pandit A. Selective removal of phosphorus from wastewater combined with its recovery as a solid-phase fertilizer. Water Res 2011;45:3318–30. https://doi.org/10.1016/j.watres.2011.03.044.
Soares A. Wastewater treatment in 2050: Challenges ahead and future vision in a European context. Environ Sci Ecotechnology 2020;2:100030. https://doi.org/10.1016/j.ese.2020.100030.

Nomenclature

$C_{L,P}$	Liquid phase concentration of PO_4-P ($mg_P\ L^{-1}$)
$C_{L,0}$, $C_{L,eq}$	Initial and final (equilibrium) PO_4-P concentration in the liquid phase (MWW or synthetic P solution) during the isotherm tests ($mg_P\ L^{-1}$ or $meq_P\ L^{-1}$)
$C_{S,eq}$	Final (equilibrium) PO_4-P concentration in the solid phase (resin) during the isotherm tests ($mg_P\ g_{dry\ resin}^{-1}$ or $meq_P\ g_{dry\ resin}^{-1}$)
$C_{S,P}$	Solid phase (resin) concentration of P ($mg_{PO4\text{-}P}\ g_{dry\ resin}^{-1}$)
$C_{S,\infty}$	maximum amount of P sorbed per unit mass of adsorbent, in the Langmuir model ($mg\ g_{dry\ resin}^{-1}$)
EBCT	Empty bed contact time, ratio between resin bed volume (mL) and flowrate (mL/min) used in the breakthrough test (min)
K_{eq}	Constant related to the affinity between the binding sites and P, in the Langmuir isotherm ($L_{pore\ volume}\ mg_P^{-1}$) and in IE model (-)
K_F	Sorption capacity in the Freundlich model ($mg_P^{1-1/n}\ L^{1/n}\ g_{dryresin}^{-1}$)
n_i	Inverse of the sorption intensity in the Freundlich model (-)
Q	Resin total capacity, asymptotic P concentration sorbed in the solid (resin) predicted by IE model ($mg_P\ g_{dry\ resin}^{-1}$ or $meq_P\ g_{dry\ resin}^{-1}$)

Regeneration and modelling of a phosphorous removal and recovery hybrid ion exchange resin after long term operation with municipal wastewater

SUPPLEMENTARY MATERIAL

Table S1
HAIX Layne^{RT}: technical properties, characterization, activation procedure and regeneration
Technical properties

Structure	Macro-porous polystirene-divinilbenzene polymer
Appearance	Brown spherical beads
Functional groups	Quaternary ammonium
Iron content	75-90 mg as Fe $g_{dry\ resin}^{-1}$
Bulk density	790-840 g L^{-1}
Particle size	180-1000 µm
Ion-exchange capacity (IE matrix)	1 meq mL^{-1}

Characterization - Layne^{RT} (SolmeteX, Massachusetts, USA) is a commercial hybrid anion exchanger principally used for arsenic removal. This media is currently marketed as Layne^{RT}, but it was previously known as FerrIX^{TM}, ArsenX^{np} and Phosx^{np}. It comprises a strong base anionic ion-exchange resin (namely a polystyrene-divinylbenzene macroporous polymer functionalised with quaternary ammonium active sites) which acts as a scaffold to support a dispersion of ferric oxide nanoparticles (Blaney et al., 2007; Cumbal et al., 2003). The internal and external surfaces of the ion-exchange (IE) resin are covered with iron nanoparticles in hydrated ferric oxide form, capable to selectively adsorb phosphate. Approximately 26% of the internal and external surfaces are covered with iron in hydrated ferric oxide form. The size of the media varies between 0.18 and 1.0 mm with a mean size of 0.69 mm (Martin et al., 2018).
Activation procedure - The virgin media was activated with the following procedure: i) a first wash with deionized (DI) water for 30 minutes, at 10 g L^{-1} of resin, stirring at 250 rpm to remove any fine iron particle left over from manufacturing; ii) a batch pre-conditioning using a 2% (w/v) NaOH solution, stirring at 250 rpm for 2 hours in order to convert the resin's form from the chloride one (in which Layne^{RT} is supplied) to the hydroxyl form; iii) a double rinse in DI water.
Regeneration procedure - The batch regeneration tests were conducted by suspending the used resin in the desorption solution with a media concentration of 10 g_{resin} $L_{solution}^{-1}$ (20-22°C, 2 h, constant stirring at 200 rpm). After desorption, a sample of the solution was analysed in terms of P and COD content. The used resin samples after separation from the desorption solution were rinsed 3 times in DI water (30 minutes, 200 rpm). The continuous regeneration tests were conducted by elution of 10 bed volumes (BVs) of the regeneration solution with an empty bed contact time (EBCT) of 10 min. Average samples of the desorption effluent were analysed. The virgin resin column was pre-treated with a NaOH solution, to change the form of the ion exchange parent media to OH^-.

Table S2
Characteristics of the wastewater used in the demonstration and lab-scale tests.

Compound	Symbol	Unit	Secondary effluent from Cranfield WWTP (Demonstration scale plant)	Final effluent from Bologna WWTP (0.17 L lab-scale column)
Ammonia nitrogen	NH_3-N	mg_N L^{-1}	5-10	5.1
Sodium	Na^+	mg L^{-1}	N.A.	136

Potassium	K^+	mg L^{-1}	N.A.	19
Magnesium	Mg^{2+}	mg L^{-1}	N.A.	25
Calcium	Ca^{2+}	mg L^{-1}	30-40	136
Phosphate	PO_4-P	Mg_P L^{-1}	5-6	1[a]
Fluoride	F–	mg L^{-1}	N.A.	0.11
Chloride	Cl–	mg L^{-1}	N.A.	150
Nitrate	NO_3^-	mg L^{-1}	32-46	6.7
Sulphate	SO_4^{2-}	mg L^{-1}	70-80	104
Biological oxygen demand	BOD_5	mg L^{-1}	N.A.	15
Chemical oxygen demand	COD	mg L^{-1}	30-40	41
Total suspended solids	TSS	mg L^{-1}	50-150	8.3
Total organic Carbon	TOC	mg L^{-1}	N.A.	7.9
pH	pH		6.5-7	7

N.A. = data not available

[a] Before conducting the lab scale tests, this effluent was spiked with a K_2HPO_4/KH_2PO_4 solution in order to attain 7 mg_P L^{-1}.

Table S3. Adsorption kinetic and isotherm tests: experimental and modelling procedures

A) Preliminary kinetic tests

The goal of the kinetic P adsorption tests was to identify the minimum time required to achieve equilibrium between the liquid and solid phase, so as to perform an optimal design of the subsequent isotherm tests. In addition, the data were used to assess the most suitable kinetic model among the most used ones: i) pseudo-first order (PFO) equation, ii) pseudo-second order (PSO) equation, iii) intra-particle diffusion equation, iv) film diffusion equation (Tran et al., 2017).

Kinetic tests were performed in 250-mL bottles according to the same operating conditions of the adsorption isotherms: initial concentration of P in the liquid phase, temperature of 20-22°C, pH around 6.9 and shaking at 200 rpm. The ratio between the mass of dry resin and the volume of liquid phase was set to 4 $g_{dry\ resin}\ L^{-1}$, on the basis of previous studies to be used for comparison (Martin et al., 2018; Zeng et al., 2004). 200 mL of solution with a P concentration of 7.0 ± 0.2 mg L^{-1} for the P-synthetic solution and of 6.0 ± 0.2 mg L^{-1} for the actual wastewater, were placed in a 250-mL bottles with 0.8 g of dry resin. Kinetic tests were conducted for both the synthetic P-solution and actual wastewater, each test was set up in triplicate. Samples were taken each 20 minutes for the first hour and then every 30 minutes up to the 6th hour. A latter point was taken after 24 h to verify that adsorption process reached true equilibrium.

The adsorption kinetic tests, aimed at asserting the adsorption equilibrium time between the liquid and solid phase, were performed both with a synthetic P solution and with the Bologna WWTP effluent (Table 2). The time required was 40 min with the synthetic solution and 90 min with the WWTP effluent, suggesting that competing ions present in the wastewater influenced the P uptake rate. These results are in agreement with the work of (Martin et al., 2018), who showed that P adsorption on Layne^{RT} is very fast: 54% of the total capacity was utilised within the first 15 min and 95% within the first 60 min. Based on these results, the equilibrium time for the subsequent isotherm tests was cautiously set at 6 h.

B) Adsorption isotherms: experimental details, model description and best fitting procedure

The resin concentration was maintained constant at 1 $g_{dry\ resin}\ L^{-1}$, the liquid volume was set to 0.1 L. For each point of the isotherms conducted with WWTP effluent, the desired P initial concentration was reached by mixing 100 mL of effluent with 0.005-1 mL aliquots of different K_2HPO_4/KH_2PO_4 solutions, so as to maintain the effect of dilution of the competing anions at negligible levels (<1%). In each added solution, the K_2HPO_4:KH_2PO_4 ratio was equal to 1:2, in order to maintain the solution pH at 6.8. These solutions were designed so as to attain a total P concentration equal to 9 g L^{-1} (for the solution added to the medium-low concentration points of the isotherms) or 90 g L^{-1} (for the solution added to the high concentration points of the isotherms).

The glass vials were placed in a rotatory shaker (200 rpm, 22°C) for 6 h, to reach the equilibrium condition. The duration of the experiment was defined based on the outcome of the above-described kinetic tests. The P equilibrium concentration in the solid phase, $C_{S,eq}$ was determined as:

$$C_{S,eq} = \frac{\left(C_{L,0} - C_{L,eq}\right) \cdot V_L}{m_S} \qquad \text{(Eq. S5)}$$

where: m_S is the mass of the dry resin, $C_{L,0}$ and $C_{L,eq}$ the initial and final PO_4-P concentration in the liquid phase and V_L the liquid volume. The tests were performed in triplicates and the 95% confidence intervals associated to $C_{S,eq}$ were calculated from the standard deviation of the mean values.

Experimental isotherms were fitted by means of the Langmuir (Eq. S6) and Freundlich (Eq. S7) models.

Langmuir $$C_{S,eq,i} = \frac{C_{S,i}^{\infty} \cdot C_{L,eq,i}}{\frac{1}{K_{eq,i}} + C_{L,eq,i}} \quad \text{(Eq. S6)}$$

Freundlich $$C_{S,eq,i} = K_{F,i} \cdot C_{L,eq,i}^{1/n_i} \quad \text{(Eq. S7)}$$

where: $C_{S,eq,i}$ (g_i $g_{dry\ resin}^{-1}$) and $C_{L,eq,i}$ ($g_i\ L^{-1}$) indicate respectively the amount of sorbed *i*-compound per unit mass of adsorbent and the *i*-compound concentration in the liquid phase at equilibrium; $C_{S,i}^{\infty}$ ($g_i\ g_{dry\ resin}^{-1}$) the maximum amount sorbed per unit mass of adsorbent, corresponding to a complete monolayer on the adsorbent surface; $K_{eq,i}$ ($L_{pore\ volume}\ mg_i^{-1}$) the constant related to the affinity between the binding sites and the *i*-compound; $K_{F,i}$ ($mg_i^{1-1/n}\ L^{1/n}\ g_{dry\ resin}^{-1}$) the sorption capacity in the Freundlich model; $1/n_i$ (-) the sorption intensity in the Freundlich model.

The model parameters were estimated by non-linear least squares regression of the calculated the *i*-compound solid phase concentrations ($C_{S,eq,calc,i}$) to the corresponding experimental values ($C_{S,eq,i}$). The best-fitting model was selected based on the correlation coefficient R^2, defined so as to take into account the number of model parameters:

$$R^2 = 1 - \left(\frac{\sum_{i=1}^{N} \left(C_{S,eq,i} - C_{S,eq,calc,i} \right)^2}{N - P - 1} \right) \Bigg/ \left(\frac{\sum_{i=1}^{N} \left(C_{S,eq,i} - C_{S,eq,m} \right)^2}{N - 1} \right) \quad \text{(Eq. S8)}$$

where N indicates the number of experimental tests in the studied isotherm, and P the number of model parameters.

In addition, the tests with the synthetic solution, where no competing anion is present, where interpolated using the ion exchange (IE) model as well. The isotherm simulation with the IE model for the exchange of a couple of ions comes from the solution of a system of 4 equations: 2 mass balances on the two ions, A (Eq. S9) and B (Eq. S10), a mass balance on the active sites in the sorbent (Eq. S11) and one equilibrium equation for the exchange reaction (Eq. S12):

$$\begin{cases} V_L \cdot C_{L,A0} + W_S \cdot C_{S,A0} = V_L \cdot C_{L,A} + W_S \cdot C_{S,A} & \text{(Eq. S9)} \\ V_L \cdot C_{L,B0} + W_S \cdot C_{S,B0} = V_L \cdot C_{L,B} + W_S \cdot C_{S,B} & \text{(Eq. S10)} \\ C_{S,A} = Q - C_{S,B} & \text{(Eq. S11)} \\ K_{eq} = \frac{C_{S,B}}{C_{L,B}} \cdot \frac{C_{L,A}}{C_{S,A}} & \text{(Eq. S12)} \end{cases}$$

Where $C_{L,A0}$ and $C_{L,B0}$ (meq L^{-1}) indicate respectively the initial concentration of ions A and B in the liquid phase during the isotherm test, $C_{S,A0}$ and $C_{S,B0}$ (meq $g_{dry\ resin}^{-1}$) the initial concentration of ions A and B in the sorbent phase, $C_{L,A}$ and $C_{L,B}$ (meq L^{-1}) the concentration in the liquid phase of ions A and B at the equilibrium, V_L (L) the liquid the volume added in the isotherm tests, W_S (g) the mass of dry resin used in the isotherm test, Q ($meq_P\ g_{dry\ resin}^{-1}$) the resin total capacity, Keq (-) the equilibrium constant of the ion exchange reaction between ions A and B.

For a complete simulation starting from $C_{L,B0}$, $C_{S,B0}$, Q, K_{eq} a second order equation is obtained. To simulate a complete isotherm, different vales of $C_{S,B}$ and $C_{L,B}$must be calculated varying the $C_{L,B0}$ in a reasonable range. The interpolation of experimental data of equilibrium liquid concentration of the ion that one wants to exchange is easier. Assuming that $C_{L,A0} = 0, C_{S,B0} = 0$, $C_{S,B}$ can be calculated

in a straightforward manner from an experimentally known $C_{L,B}$ solving by substitution from the following three equation system:

$$\begin{cases} C_{L,A} = C_{L,B0} - C_{L,B} & (\text{Eq. S13}) \\ C_{S,A} = Q - C_{S,B} & (\text{Eq. S14}) \\ K_{eq} = \dfrac{C_{S,B}}{C_{L,B}} \cdot \dfrac{C_{S,A}}{C_{L,A}} & (\text{Eq. S15}) \end{cases}$$

The explicit equation useful for the calculation of $C_{S,B}$ from an experimentally known $C_{L,B}$is:

$$C_{S,B} = \frac{K_{eq} \cdot C_{L,B} \cdot Q}{C_{L,B0} - C_{L,B} + K_{eq} \cdot C_{L,B}} \qquad (\text{Eq. S16})$$

The best-ft parameters of the model are K_{eq} and the total capacity of the resin (Q).

Table S4. Laboratory adsorption column packing and packing quality assessment

The column used for the lab-scale breakthrough tests had a total height of 1.26 m, and a resin bed height of 0.94 m as in the 58-L demonstration plant. The column total volume resulted 0.167 L. The inner diameter was set to 13 mm, a compromise between the requirement to maintain the (inner diameter)/(mean particle size) ratio > 12 to ensure a correct fluid-dynamic behaviour (Inamuddin and Luqman, 2012) and the need to minimize the WWTP effluent flow rate, and consequently the amount of WWTP effluent that had to be sampled and transferred to the laboratory for each breakthrough test. The above-justified choice of a relatively small column diameter (13 mm), combined with the selection of a resin bed height typical of industrial applications (940 mm) resulted in a value of the (resin bed height / inner diameter) ratio equal to 940/13 = 72.3. This value is higher than that typical of industrial applications, but in line with the literature recommendation of a ratio > 5 to ensure a correct fluid-dynamic behavior (Inamuddin and Luqman, 2012).

The column packing was achieved by first placing a 60 mm layer of gravel and quartz sand at the bottom. Then, the column was filled by repeatedly adding 20 mL of wet resin and then waiting for the settling before adding the next amount. DI water was fed to help resin beads to settle and compact during the packing. The final resin bed height was equal to that of the 58 L adsorption column (0.94 m). The residual 0.26 m on the top of the column were filled with water to let space for resin swelling and partial fluidization during the backwashing of the bed.

As a preliminary step, a fluid-dynamic analysis was performed on the adsorption columns packed with the three resins tested in the isotherm batch tests: virgin resin, used resin regenerated with NaOH and used resin regenerated with NaOH/NaCl. Conventional frontal analysis tests were conducted by flowing DI water after having conditioned the column with a 0.5M NaOH solution. Three tests were conducted for each adsorption bed at different superficial velocities: 3.4, 7.1 and 10.5 m h^{-1}. The latter velocity corresponds to an EBCT of 5.4 min, close to that applied in the continuous adsorption breakthrough tests. Electrical conductivity was measured at the column outlet with an EUTECH Instruments 2700 series conductometer (ThermoFisher Scientific, Walthman, Massachusetts, USA).

The packing quality was evaluated by means of three indicators: i) height equivalent of a theoretical plate (HETP), ii) reduced plate height h ($HETP/d_p$ where d_p is the mean diameter of the particles) and iii) asymmetry factor (A_s), defined as the ratio between the leading and tailing semi-width of the peak at 10% of the peak height, and representing the peak deviation from a Gaussian peak. The procedure for the evaluation of these indicators is described by (Frascari et al., 2016).

Table S5. Long-term operation of the 58 L P recovery column

Fig. S1a presents the profiles of P concentration in the effluent after treatment with HAIX during the last 10 cycles of the total 63 cycles performed at demonstration scale in the 58 L plant. Even after 63 cycles, it was possible to maintain the effluent concentration below 0.1 $mg_P\ L^{-1}$ after regeneration, indicating that HAIX can be used for long-term operation. According to literature, the HAIX adsorption capacity can range between 0.29 and 14.4 mg PO_4-P $g_{dry\ resin}^{-1}$, depending on the initial PO_4-P wastewater concentration (Bottini and Rizzo, 2012; Muhammad et al., 2019). In this work, with an influent concentration of 5-6 $mg_P\ L^{-1}$, the resin presented a maximum adsorption capacity of around 4.1 ± 0.4 $mg_P\ g_{dry\ resin}^{-1}$, working at an EBCT of 5 minutes.

However, the prolonged use of the resin decreased the amount of bed volumes treated before breakthrough. Fig. S1b shows a comparison between cycle 1 and cycle 59. In cycle 1, an effluent concentration <0.25 $mg_P\ L^{-1}$ was maintained for 432 bed volumes, whereas in cycle 59, the same concentration was maintained for 132 bed volumes indicating a gradual decrease in the adsorption capacity of the resin. During the entire period of operation, 11 batches of fresh NaOH solution used as regenerant were prepared. The regenerant solution was replaced with a fresh one when the regeneration efficacy was no longer acceptable. Overall, the regenerant was reused up to 8 times with a final concentration of around 800 $mg_P\ L^{-1}$ (Figure S1c). On average, around 51% of the adsorbed PO_4-P was recovered in the regenerant solution, corresponding to a desorption capacity of 2.1 ± 0.7 $mg_P\ g_{dry\ resin}^{-1}$.

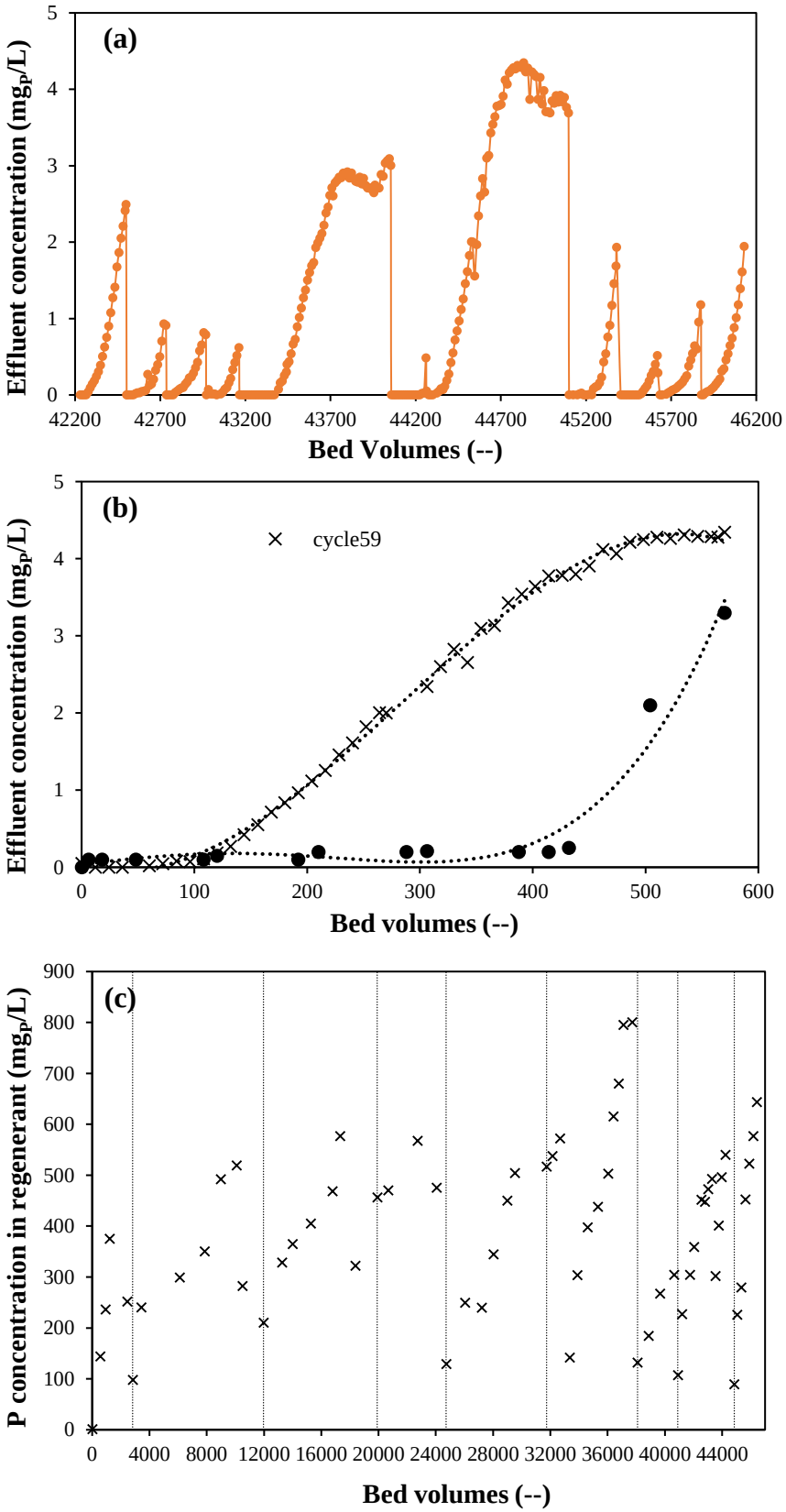

Figure S1 - Long-term operation of HAIX for P removal during 63 adsorption / desorption cycles. (a) Effluent profiles of cycles 52-63 at demonstration scale; (b) breakthrough curves at cycle 1 and 59; (c) PO_4-P concentration in regenerant (fresh batches of regenerant are indicated with vertical line).

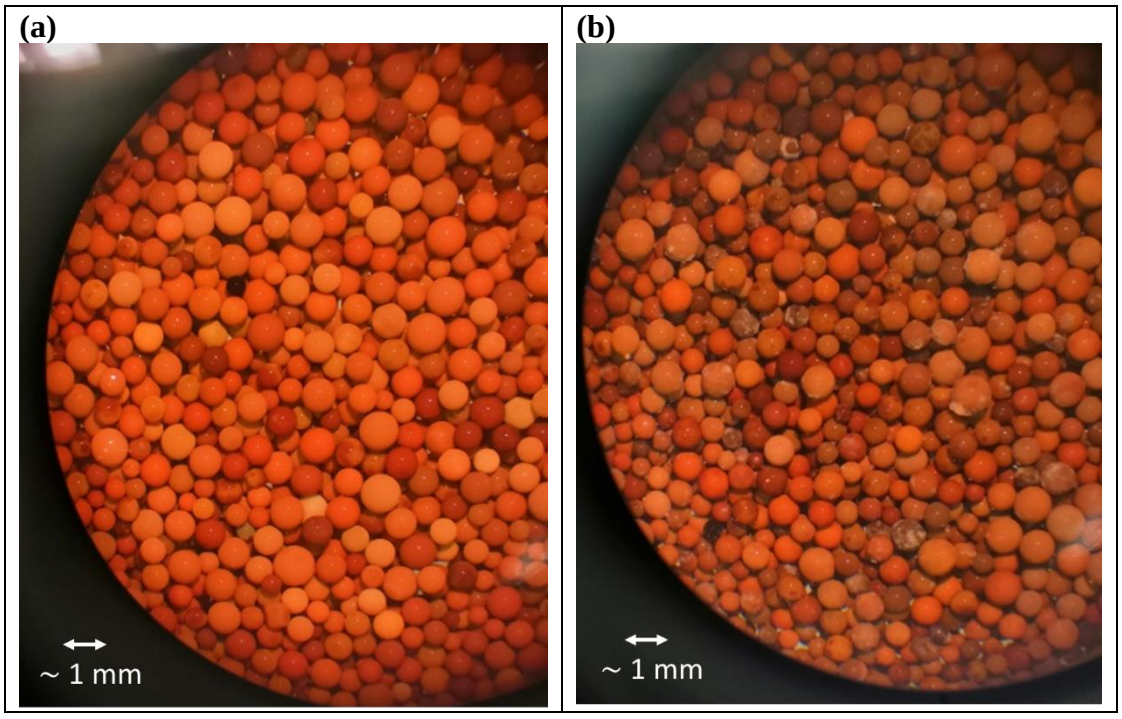

Figure S2. (a) Virgin Layne^{RT} and (b) used resin after 16 adsorption / desorption cycles analysed at the optical microscope**.**

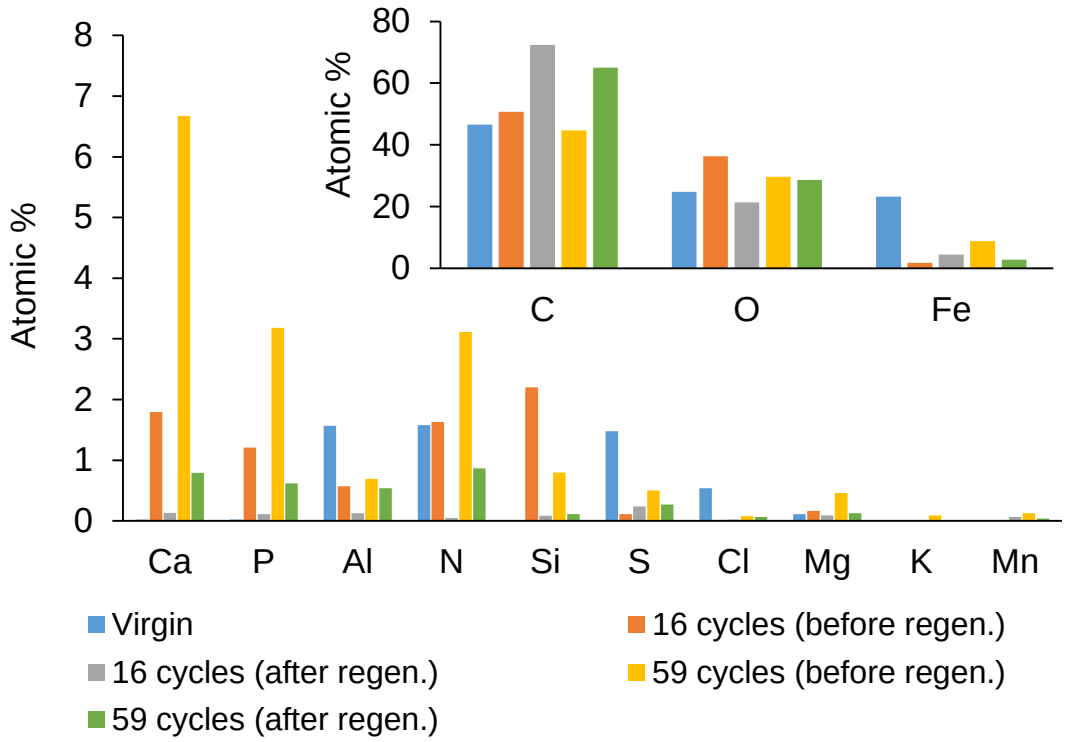

Figure S3. Scanning electron microscopy analysis of virgin and used Layne^{RT} resin after 16 and 59 adsorption /desorption cycles, before and after regeneration with NaOH.

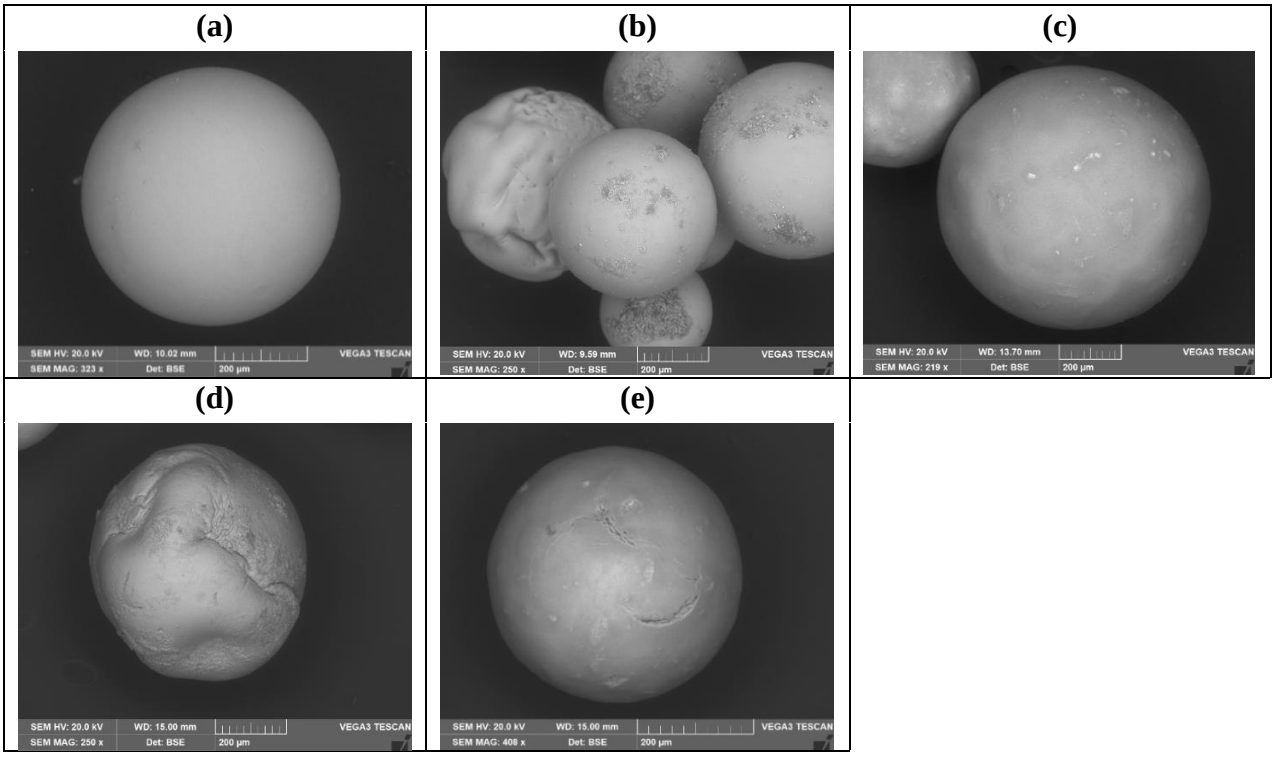

Figure S4. Scanning electron microscopy analysis of the resin surface: (a) virgin resin; used resin after 16 cycles (b) before and (c) after regeneration; used resin after 59 cycles (d) before and (e) after regeneration

Table S6 – Amounts of P and COD desorbed from the used Layne^{RT} resin after 63 adsorption / desorption cycles conducted with actual WWTP effluent: comparison between different types of regeneration procedures.

	Regeneration with NaOH 2%		Regeneration with NaOH 2% + NaCl 5%	
	Batch mode	Continuous flow mode[a]	Batch mode	Continuous flow mode[a]
P desorbed ($mg_P\ g_{dry\ resin}^{-1}$)	3.9 ± 0.3	5.2 ± 0.1	4.6 ± 0.3	5.3 ± 0.1
COD desorbed ($mg_{COD}\ g_{dry\ resin}^{-1}$)	6 ± 1	4 ± 1	97 ± 5	75 ± 5

[a] Operational conditions: EBCT 10 minutes; superficial velocity 7.6 m h^{-1}; BVs of regenerant solution eluted: 10.

Table S7 – Kinetic tests of P adsorption on Layne^{RT}: discussion of the results

Experimental data were interpolated by non-linear least squares using the four following equations (Tran et al., 2017):

1) Pseudo-first-order (PFO) equation:

$$C_S = C_{S,eq}\,(1 - e^{k_1 t}) \quad \text{(Eq. S1)}$$

where $C_{S,eq}$ (mg g^{-1}) and C_S (mg g^{-1}) are the amounts of adsorbate uptake per mass of adsorbent at equilibrium and at any time t (min), respectively; and k_1 (min^{-1}) is the rate constant of the PFO equation.

2) Pseudo-second-order (PSO) equation:

$$C_S = \frac{C_{S,eq}^2\, k_2 t}{1 + C_{S,eq} k_2 t} \quad \text{(Eq. S2)}$$

where $C_{S,eq}$ (mg g^{-1}) and C_S (mg g^{-1}) are the amount of adsorbate adsorbed at equilibrium and at any t (min), respectively; and k_2 (g/(mg min)) is the rate constant of the PSO equation.

Generally, although the PSO model can adequately describe adsorption kinetic test adsorption kinetic experimental data, this model does not reveal the adsorption mechanisms. In order to have an insight into the reaction pathways and the adsorption mechanisms the two following equations were applied (Martin et al., 2018):

3) Intra-particle diffusion equation:

$$C_S = k_{IP}\, t^{0.5} \quad \text{(Eq. S3)}$$

where C_S (mg g^{-1}) is the amount of adsorbate adsorbed at any t (min) and k_{IP} (mg g^{-1} min$^{-0.5}$) is the rate constant.

4) Film diffusion equation:

$$\ln(1 - F) = -k_{FD}\, t \quad \text{(Eq. S4)}$$

where F is the fractional attainment of equilibrium at any t (min) and k_{FD} (min^{-1}) is the rate constant.

To calculate the kinetic parameters, nonlinear methods were applied, in according to what recommended by many researchers (Tran et al., 2017). Furthermore, to identify the best-fitting model, the chi-squared (χ^2) value was calculated in addition to the coefficient of determination (R^2) for the nonlinear method. In the chi-squared test, the squares of the differences between the experimental data and data calculated using the models are divided by the corresponding data obtained and then summed. If the data obtained using a model are similar to the experimental data, χ^2 is close to zero. High χ^2 values indicate a high bias between the experimental data and the model (Tran et al., 2017).

The R^2 was calculated as indicated in Tab. S3.

The kinetics of P adsorption on HAIX Layne^{RT} resulted to be best described by the pseudo-first order model, even if also the pseudo-second order and film diffusion models resulted in very high R^2 values. The kinetic parameters relative to the intra-particle diffusion model are not reported, as this model resulted not suitable at all for the interpolation of the experimental data. The pseudo-first order constants obtained both with the synthetic solution and the actual WWTP effluent are of the same order of magnitude of those reported by (Pan et al., 2009) for an HAIX sorbent very similar to Layne^{RT} ($2.4 – 2.7 \cdot 10^{-2}$ min^{-1}). To assess whether P adsorption on Layne^{RT} is controlled by only film diffusion in the particle external boundary layer or by the combined effect of film diffusion and intra-particle pore diffusion, P concentrations in the solid were plotted against $t^{0.5}$. The trend was not linear, suggesting that adsorption is not controlled by intra-particle diffusion, but by a multistep mechanism (Tran et al., 2017). This result agrees with the conclusions of (Martin et al., 2018), who found that both film and intra-particle diffusion are relevant for P adsorption on Layne^{RT}.

Conversely, intra-particle diffusion dominates as rate-controlling mechanism in several commonly used adsorbents characterized by a macroporous structure, such as activated carbon (Cooney, 1998).

Table S8. Kinetic tests of P adsorption on virgin Layne^{RT} resin performed with synthetic P solution and actual effluent of the Bologna WWTP: best fitting values of the model parameters relative to the interpolation performed with the models illustrated in Table S7.

Model	Parameter	Units	Kinetic test with synthetic P-solution	Kinetic test with effluent of the Bologna WWTP
Psuedo-1st order	k_1	min^{-1}	0.153	0.095
	$C_{S,eq}$	$mg_P\ g_{dry\ resin}^{-1}$	1.485	1.724
	R^2	--	0.99998	0.99998
Psuedo-2nd order	k_2	$g_{dry\ resin}\ (mg_P\ min)^{-1}$	0.539	0.123
	$C_{S,eq}$	$mg_P\ g_{dry\ resin}^{-1}$	1.509	1.822
	R^2	--	0.99980	0.99851
Film diffusion	k_{FD}	min^{-1}	0.148	0.090
	R^2	--	0.99992	0.99921

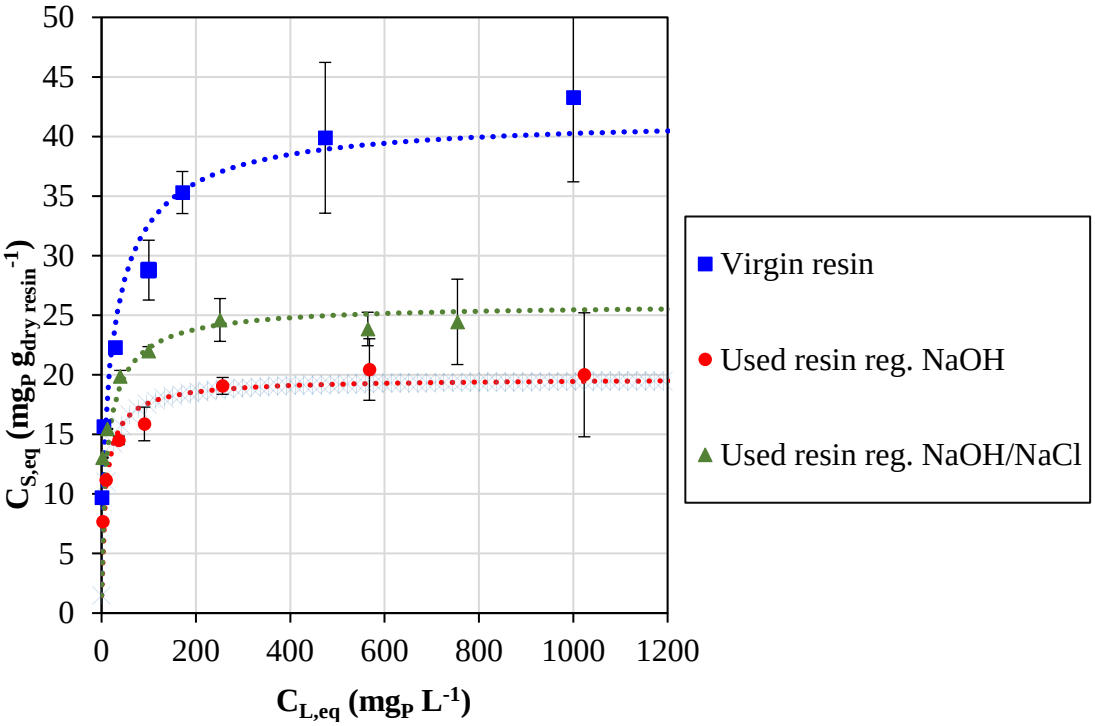

Figure S5. Isotherms conducted with synthetic solution and Layne^{RT} resin: best-fitting interpolation obtained with the ion exchange model (Table S3, Eqs. S9-S12)

Table S9. Laboratory adsorption column fluid-dynamic analyses

The packing quality was evaluated by means of three indicators: i) height equivalent of a theoretical plate (HETP), ii) reduced plate height h ($HETP/d_p$ where d_p is the mean diameter of the particles) and iii) asymmetry factor (A_s), defined as the ratio between the leading and tailing semi-width of the peak at 10% of the peak height, and representing the peak deviation from a Gaussian peak. The procedure for the evaluation of these indicators is described by (Frascari et al., 2016).

The analysis of the packing quality resulted in an average asymmetry factor of the retention time distribution curve equal to 1.7 ± 0.3, and an average reduced plate height equal to 65 ± 8. These values are considered acceptable for columns packed with adsorption resins.

Overall, the fluid-dynamic analysis indicates that (i) the aging of the Layne^{RT} resin did not determine any relevant variation in the packing quality and in the resulting resin porosity, and (ii) despite the 17-fold reduction in column diameter in comparison to the 58 L pilot plant, the lab-scale continuous flow adsorption / desorption tests were conducted in a column characterized by an acceptable fluid-dynamic behaviour.

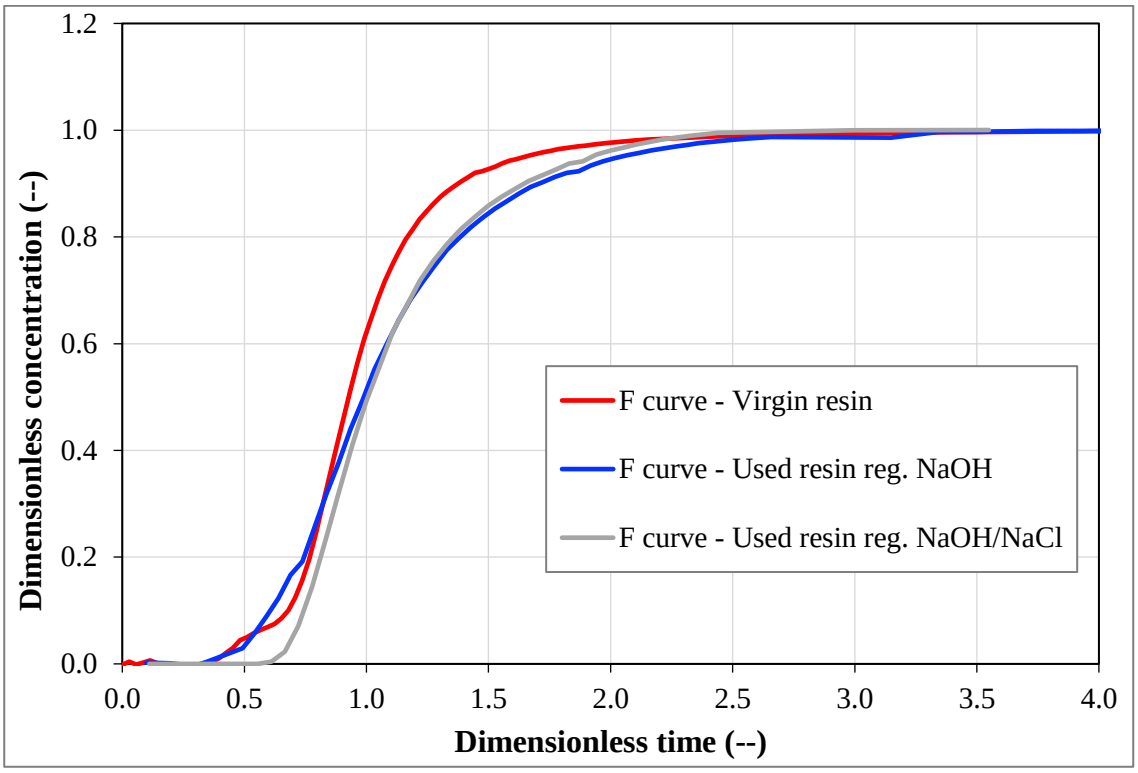

Figure S6. Cumulative retention time curves obtained in the frontal analysis tests performed with in the columns packed with the virgin Layne^{RT} resin, with the used resin regenerated with NaOH and with the used resin regenerated with NaOH/NaCl. Tests performed at a superficial velocity of 7.1 m h^{-1}.

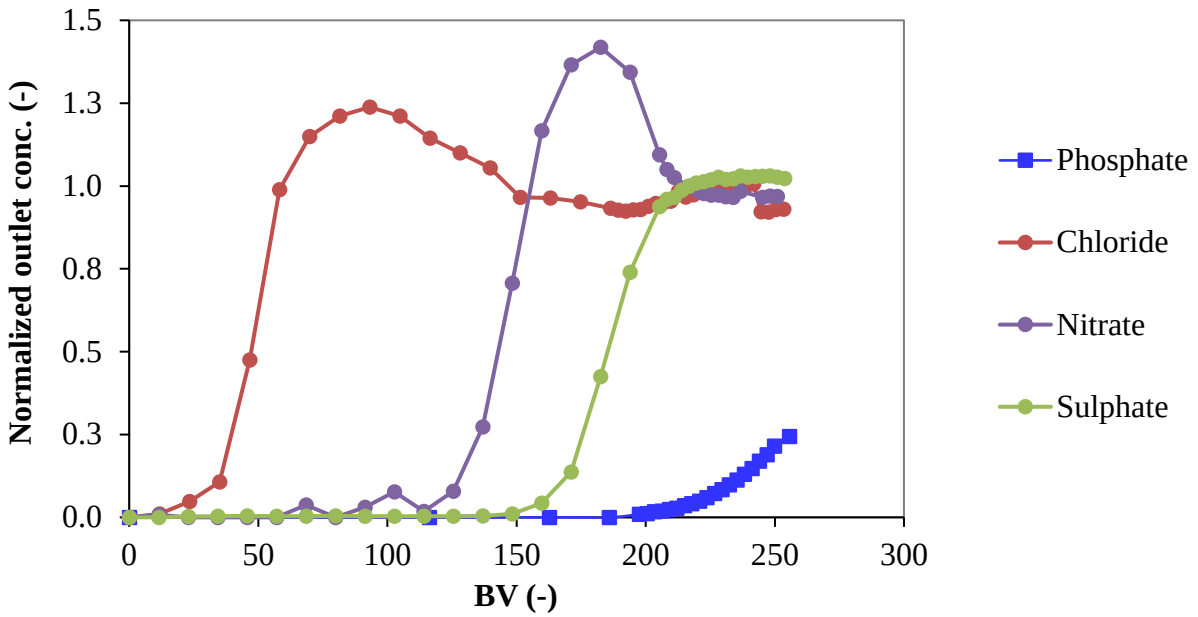

Figure S7. Breakthrough curves of phosphate and the competing anions obtained with P-spiked WWTP effluent and the used resin regenerated with NaOH, in the 0.167 column. The operating conditions are shown in Table 5. Anions inlet concentrations were: phosphate 6.6 $mg_P\ L^{-1}$, chloride 150 $mg\ L^{-1}$, nitrate 6.7 $mg\ L^{-1}$ and sulphate 104 $mg\ L^{-1}$.

Table S10. Desorption continuous flow tests: discussion of the results.

Overall, the results of the adsorption / desorption tests (Table 6) indicate that the 2 types of regenerated Layne^{RT} resulted about equal to the virgin resin in terms of capacity to retain P and concentrate it in the desorbed product.

In the perspective to use the desorbed product for the production of a P-rich fertilizer, the relatively low P content of the product does not represent a concern, as P can be easily separated by precipitation as $Ca_3(PO_4)_2$ following the addition of $Ca(OH)_2$ to the desorbed product. This final step is beyond the scope of this work, focused on the comparison of the P adsorption behaviour and performances of the 3 forms of Layne^{RT}.

The amounts of anions measured in the desorbed product where used to assess the total anion adsorption capacity and the P adsorption capacity of the 3 forms of Layne^{RT} (Table 6). The total capacity of the NaOH/NaCl-regenerated resin (2.1 $meq_P\ g_{dry\ resin}^{-1}$) resulted slightly higher, but not statistically different (t test, 0.05 significance level) than that of the virgin resin (2.0 $meq_P\ g_{dry\ resin}^{-1}$), whereas the total capacity of the NaOH-regenerated Layne^{RT} was 15% lower and statistically different than that of the virgin Layne^{RT}. As shown in Table 6, these desorption-based estimates of the Layne^{RT} total capacity are in reasonable agreement with those obtained from the isotherm tests conducted with the "clean" synthetic solution, that represent the best way to estimate the total capacity in the absence of anion competition.

As for the desorption-based estimates of the P adsorption capacity, the values obtained for the two regenerated resins (0.38-0.41 $meq_P\ g_{dry\ resin}^{-1}$) resulted slightly lower, but not statistically different, than those relative to the virgin Layne^{RT} (0.42 $meq_P\ g_{dry\ resin}^{-1}$). Similarly, the estimates of the P adsorption capacity at the 1 $mg_P\ L^{-1}$ breakpoint obtained from the adsorption test with the two regenerated resins (0.33-0.38 $meq_P\ g_{dry\ resin}^{-1}$) resulted very close, and not statistically different, to the corresponding estimate obtained for the virgin resin (0.35 $meq_P\ g_{dry\ resin}^{-1}$; Table 6). Likewise, the evaluations of the P adsorption capacity at 7 $mg_P\ L^{-1}$ in the liquid phase obtained from the isotherms conducted with actual WWTP effluent with the two regenerated resins (0.24-0.30 $meq_P\ g_{dry\ resin}^{-1}$) resulted lower but not statistically different than the corresponding value obtained for the virgin resin (0.39 $meq_P\ g_{dry\ resin}^{-1}$; Table 6). The comparison between the P capacities obtained from the adsorption test at the 1 $mg_P\ L^{-1}$ breakpoint and those obtained from the isotherms at 7 $mg_P\ L^{-1}$ in the liquid is based on the observation that – in continuous flow tests with a narrow mass transfer zone as those conducted in the 0.167 columns – when the effluent reaches the 1 $mg_P\ L^{-1}$ breakpoint, most of the resin bed is in equilibrium with liquid at the inlet P concentration, equal to about 7 $mg_P\ L^{-1}$ (Table 5).

References cited in the Supplementary Materials

Blaney, L.M., Cinar, S., SenGupta, A.K., 2007. Hybrid anion exchanger for trace phosphate removal from water and wastewater. Water Res. 41, 1603–1613. https://doi.org/10.1016/j.watres.2007.01.008

Bottini, A., Rizzo, L., 2012. Phosphorus Recovery from Urban Wastewater Treatment Plant Sludge Liquor by Ion Exchange. Sep. Sci. Technol. 47, 613–620. https://doi.org/10.1080/01496395.2011.627904

Cooney, D.O., 1998. Adsorption Design for Wastewater Treatment. CRC Press, Florida.

Cumbal, L., Greenleaf, J., Leun, D., SenGupta, A.K., 2003. Polymer supported inorganic nanoparticles: Characterization and environmental applications. React. Funct. Polym. 54, 167–180. https://doi.org/10.1016/S1381-5148(02)00192-X

Frascari, D., Bacca, A.E.M., Zama, F., Bertin, L., Fava, F., Pinelli, D., 2016. Olive mill wastewater valorisation through phenolic compounds adsorption in a continuous flow column. Chem. Eng. J. 283, 293–303. https://doi.org/10.1016/j.cej.2015.07.048

Inamuddin D, Luqman M, 2012. Ion Exchange Technology I - Theory and Materials. Springer Netherlands, p 136.

Martin, B.D., De Kock, L., Gallot, M., Guery, E., Stanowski, S., MacAdam, J., McAdam, E.J., Parsons, S.A., Jefferson, B., 2018. Quantifying the performance of a hybrid anion exchanger/adsorbent for phosphorus removal using mass spectrometry coupled with batch kinetic trials. Environ. Technol. (United Kingdom) 39, 2304–2314. https://doi.org/10.1080/09593330.2017.1354076

Muhammad, A., Soares, A., Jefferson, B., 2019. The impact of background wastewater constituents on the selectivity and capacity of a hybrid ion exchange resin for phosphorus removal from wastewater. Chemosphere 224, 494–501. https://doi.org/10.1016/j.chemosphere.2019.01.085

Pan, Bingjun, Wu, J., Pan, Bingcai, Lv, L., Zhang, W., Xiao, L., Wang, X., Tao, X., Zheng, S., 2009. Development of polymer-based nanosized hydrated ferric oxides (HFOs) for enhanced phosphate removal from waste effluents. Water Res. 43, 4421–4429. https://doi.org/10.1016/j.watres.2009.06.055

Tran, H.N., You, S.-J., Hosseini-Bandegharaei, A., Chao, H.-P., 2017. Mistakes and inconsistencies regarding adsorption of contaminants from aqueous solutions - A critical review. Water Res. 120, 88–119. https://doi.org/10.1016/j.watres.2017.04.014

Zeng, L., Li, X., Liu, J., 2004. Adsorptive removal of phosphate from aqueous solutions using iron oxide tailings. Water Res. 38, 1318–1326. https://doi.org/10.1016/j.watres.2003.12.009

Nomenclature

A_s	Asymmetry factor, defined as ratio between the leading and tailing semi-width of the peak at 10 % of the peak height (-)
$C_{L,P}$	Liquid phase concentration of PO_4-P ($mg_{PO4\text{-}P}\ L^{-1}$)
$C_{L,0}$, $C_{L,eq}$	Initial and final (equilibrium) PO_4-P concentration in the liquid phase (MWW or synthetic P solution) during the isotherm tests (mg_P/L or $meq_P\ L^{-1}$)
$C_{S,eq}$	Final (equilibrium) PO_4-P concentration in the solid phase (resin) during the isotherm tests ($mg_P\ g_{dry\ resin}^{-1}$ or $meq_P\ g_{dry\ resin}^{-1}$)
$C_{S,P}$	Solid phase (resin) concentration of P ($mg_{PO4\text{-}P}\ g_{dry\ resin}^{-1}$)
$C_{S,\infty}$	maximum amount of P sorbed per unit mass of adsorbent, in the Langmuir model ($mg_P\ g_{dry\ resin}^{-1}$)
d_P	Average resin particles diameter (mm)
EBCT	Empty bed contact time, ratio between resin bed volume (mL) and flowrate (mL min^{-1}) used in the breakthrough test (min)

EBV	Empty bed volumes, ratio between experimental time (min) and EBCT (-)
h	Reduced plate height, defined as ratio between HETP and d_P
HETP	Height equivalent to a theoretical plate, in the packed column (m)
K_{eq}	Constant related to the affinity between the binding sites and P, in the Langmuir isotherm ($L_{pore\ volume}$ /mg_P) and in IE model (-)
K_F	Sorption capacity in the Freundlich model ($mg_P^{1-1/n}\ L^{1/n}\ g_{dryresin}^{-1}$)
m_S	Mass of dry resin in the isotherm studies ($g_{dry\ resin}$)
n_i	Inverse of the sorption intensity in the Freundlich model (-)
Q	Resin total capacity, asymptotic P concentration sorbed in the solid (resin) predicted by IE model ($mg_P\ g_{dry\ resin}^{-1}$ or $meq_P\ g_{dry\ resin}^{-1}$)
V_L	Liquid volume added in the isotherm tests (mL)
v_{sup}	Superficial velocity breakthrough test ($m\ h^{-1}$)
Y_{des}	*P* desorption yield in breakthrough tests, defined as desorbed and adsorbed mass of P (-)
%wt	Weight/Volume Percentage Concentration ($g\ L^{-1}$)